

Duality Cascade in Brane Inflation

Rachel Bean^{1*}, Xingang Chen^{2,3†}, Girma Hailu^{4‡}, S.-H. Henry Tye^{3,4§} and Jiajun Xu^{3,4¶}

¹Department of Astronomy, Cornell University, Ithaca, NY 14853, USA

²Center for Theoretical Physics,

Massachusetts Institute of Technology, Cambridge, MA 02139, USA

³Kavli Institute for Theoretical Physics in China,
Chinese Academy of Science, Beijing 100080, P.R.China

⁴Newman Laboratory for Elementary Particle Physics,
Cornell University, Ithaca, NY 14853, USA

ABSTRACT: We show that brane inflation is very sensitive to tiny sharp features in extra dimensions, including those in the potential and in the warp factor. This can show up as observational signatures in the power spectrum and/or non-Gaussianities of the cosmic microwave background radiation (CMBR). One general example of such sharp features is a succession of small steps in a warped throat, caused by Seiberg duality cascade using gauge/gravity duality. We study the cosmological observational consequences of these steps in brane inflation. Since the steps come in a series, the prediction of other steps and their properties can be tested by future data and analysis. It is also possible that the steps are too close to be resolved in the power spectrum, in which case they may show up only in the non-Gaussianity of the CMB temperature fluctuations and/or EE polarization. We study two cases. In the slow-roll scenario where steps appear in the inflaton potential, the sensitivity of brane inflation to the height and width of the steps is increased by several orders of magnitude comparing to that in previously studied large field models. In the IR DBI scenario where steps appear in the warp factor, we find that the glitches in the power spectrum caused by these sharp features are generally small or even unobservable, but associated distinctive non-Gaussianity can be large. Together with its large negative running of the power spectrum index, this scenario clearly illustrates how rich and different a brane inflationary scenario can be when compared to generic slow-roll inflation. Such distinctive stringy features may provide a powerful probe of superstring theory.

*rbean@astro.cornell.edu

†xgchen@mit.edu

‡hailu@lepp.cornell.edu

§tye@lepp.cornell.edu

¶jx33@cornell.edu

Contents

1. Introduction	2
2. The Model	6
3. The Power Spectrum and Bispectrum in General	9
4. Steps in Slow-Roll Brane Inflation	11
4.1 The Position of the Steps	11
4.2 The Power Spectrum	12
4.3 Non-Gaussianities	14
5. Steps in IR DBI Inflation	16
5.1 The Properties of the Steps	16
5.2 Qualitative Analyses around a Single Step	18
5.2.1 The Evolution of the Sound Speed	18
5.2.2 The Power Spectrum	20
5.2.3 Non-Gaussianities	22
5.3 An Analytical Approximation for a Single Sharp Step	23
5.4 Numerical Analyses and Data Fitting	25
5.5 Closely Spaced Steps	29
6. Remarks	29
A. The Warp factor	30
B. The z''/z in Slow Roll Case	32
C. Estimate the width of the steps	33
C.1 The width from Seiberg duality	33
C.2 The width from multiple brane spreading	34

1. Introduction

It is generally believed that the early universe went through an inflationary epoch [1]. In the field theory context, the most studied realization is the slow-roll inflationary scenario [2]. Such models confront primordial cosmological observation via two data points : the magnitude of the density perturbation (or temperature fluctuation in the cosmic microwave background radiation (CMBR)) as measured by COBE [3] $\delta_H \sim 10^{-5}$, and the approximately scale invariant scalar power spectrum, with index $n_s \sim 1$. In addition, there are three observational upper bounds on, namely, the tensor to scalar ratio $r < 0.3$, the running of the spectral index $|dn_s/d \ln k| < 0.1$ and the non-Gaussianity $f_{NL} < \mathcal{O}(100)$ [4, 5]. Typical predictions of $dn_s/d \ln k$ and f_{NL} (and maybe even r) may very well be far too small to be detected. Since the COBE normalization typically fixes the scale of the model, so far, the deviation of n_s from unity is the only parameter that discriminates among slow-roll inflationary models. It is not surprising, therefore, that present data allows a large degeneracy of models [6].

If superstring theory is correct, it must provide an inflationary scenario for the early universe. It should provide a precise and restrictive framework for inflationary model building while at the same time, new scenarios and new phenomena are likely to appear. Hopefully it will predict distinctive stringy signatures that, if observed, can be used to support superstring theory. It is along this direction that this paper attempts to address. Here we like to discuss the possibility of a stringy feature that may show up in a distinctive fashion in the CMBR. If the proposal is realized in nature, the number of data points linking theory and cosmological observation may increase (from ~ 2) by as much as an order of magnitude, substantially strengthening the test of inflation as well as the specific stringy realization of inflation.

It has become clear that the brane inflationary scenario is quite natural in string theory [7]. Here, the inflaton is simply the position of a mobile brane in the compactified bulk [8, 9]. In flux compactification in Type IIB string theory, where all closed string moduli are dynamically stabilized, warped geometry appears naturally in the compactified bulk [10]. Warped geometry in the 6-dimensional compactified bulk tends to appear as warped throats. In the simple but realistic scenarios, inflation takes place as $D3$ -branes move up or down a warped throat [11, 12, 13]. Inflation typically ends when the $D3$ -branes reach the bottom of a throat and annihilate the anti- $D3$ -branes sitting there. The energy released heats up the universe and starts the hot big bang.

The warped geometry either shifts masses to the infrared and helps to flatten the inflaton potential, or provides speed-limit that restricts the inflaton velocity, thus improving the e-folds of inflation. A typical throat is a warped deformed (or resolved) conifold. A string scale test mass in the bulk is red-shifted to a smaller value at the bottom of the throat. Via gauge/gravity duality, moving down the throat corresponds to a gauge theory flowing towards the infrared region. The best known example suitable for brane inflation is the $\mathcal{N} = 1$ supersymmetric Klebanov-Strassler (KS) throat in type IIB string theory on approximate $AdS_5 \times T^{1,1}$ background [14]. It is argued that the KS throat is dual to the $\mathcal{N} = 1$ supersymmetric $SU(N + M) \times SU(N)$ (with $N = KM$) gauge theory with

bifundamental chiral superfields and a quartic tree level superpotential in four dimensions [15, 16]. As the gauge theory flows towards the infrared, $SU(N + M) = SU((K + 1)M)$ becomes strongly coupled and Seiberg “electric-magnetic” duality says that it is equivalent to a weakly coupled $SU((K - 1)M)$ with appropriate matter content [17]. As a result, the gauge theory becomes $SU((K - 1)M) \times SU(KM)$ with the same set of bifundamentals. This process repeats as the gauge theory continues its flow towards the infrared; that is, it goes through a series of Seiberg duality transitions. This is known as the duality cascade [18].

Recently, a more detailed analysis of this Seiberg duality cascade [19] shows that there are corrections to the anomalous mass dimensions and their effects in the renormalization group flow of the couplings on the gauge theory side show up as small structures on the supergravity side: as steps appearing in the warped metric. The steps in the warp factor are expected to be slightly smoothed out, leading to a cascade feature that may be observable in cosmology. It was conjectured in Ref.[19] that the origin of the steps might be localized charges (branes) at radial positions inside the throat. To fully understand the gravity dual of the duality cascade, one needs to take the branes into account and study the resulting supergravity solutions together with the thickness and the stability of the branes including other smooth corrections to the KS solution. We leave this issue for future study and in this paper we focus only on the observable effects due to the steps. The presence of steps is quite generic: either as a correction to the approximate geometry for a warped throat, or as a variation of the simplest warped deformed throat in the KKLMNT-like scenario. Although the KS throat is the best understood example, in some sense it is too simple, i.e., there are no chiral fields in the infrared. Warped throats are natural consequences of flux compactification. They arise by considering Calabi-Yau singularities that admit complex deformations, corresponding to smoothing the singular points with 3 cycles on which to turn on fluxes. The holographic duals are given by duality cascades of gauge theories on D3-branes at the singular geometries. Generically, steps due to jumps in magnitudes of anomalous mass dimensions appear. Each duality cycle contains a number of steps (the KS throat has only one step in each cycle). Such steps can introduce sharp features in the cosmic microwave background radiation. Such a step may have been observed already [4, 5]. In general, a $D3$ brane encounters many steps as it moves inside a throat. If the steps are close enough, as expected, the power spectrum may be changed little, but the impact on the non-Gaussianity can be large. The duality cascade behavior of the warped geometry can therefore have distinct observable stringy signatures in the cosmic microwave background radiation. The possibility of detecting and measuring the duality cascade is a strong enough motivation to study the throat more carefully. Although both Seiberg duality and gauge/gravity duality are strongly believed to be true, neither has been mathematically proven; so a cosmological test is highly desirable. This will also provide strong evidence for string theory.

It was proposed that one can easily envision a multi-warped throat, that is, a throat inside another throat (i.e., the IR of one throat is matched to the UV of another throat) [20]. Here we expect a kink in the warp factor, but not a step. Again, we expect this to generate some non-Gaussianity.

Here we discuss the generic features introduced by the presence of such steps in the warped geometry of a throat. We consider the presence of steps in both slow-roll and DBI inflation. To be general, we shall allow the steps to go either up or down and we consider both cases. Their properties can be quite different in these scenarios. However, some features can be quite independent of details. For example, as an illustration, let us assume the feature in WMAP CMBR data at $l \simeq 20$ (with width about $\delta l \simeq 10$) is due to such a step. If we further assume that the deviation around $l \simeq 2$ is at least partly due to another step (i.e., not all due to cosmic variance), then we can predict that its width $\delta l \simeq 2$. Furthermore, we would then expect additional steps at $l \simeq 200$ (with width $\delta l \simeq 100$) and $l \simeq 2000$ (with width $\delta l \simeq 1000$) and so on. However, the sizes of the steps are more model dependent, though they tend to vary monotonically. If there is no step at $l \sim 2$, then the next step is expected at some $l > 200$.

As illustrations, we consider two specific scenarios:

1. Its properties in slow-roll brane inflation. Effects of steps on power spectrum in CMBR in slow-roll inflation have already been studied in inflationary models [21, 22, 23, 24] and in details [25, 26, 27] in chaotic inflation. Its effect on the non-Gaussianity has also been studied in details in Ref. [28, 29]. Assuming that the $l \sim 20$ feature is due to a step, Ref. [28] shows that the non-Gaussianity in chaotic-like inflation gives $f_{NL}^{\text{feature}} \sim \mathcal{O}(10)$. Because the shape and running of this non-Gaussianity is distinctively different from the cases done in data analysis, whether the PLANCK satellite is going to be able to test it remains an open question. In slow-roll brane inflation, the inflaton, being the position of the brane, is bounded by the size of the flux compactification volume, and so typically $\phi \ll M_{\text{pl}}$, as opposed to large field case for chaotic inflation, where the inflaton takes values much larger than the Planck mass ($\phi \geq 15M_{\text{pl}}$). Consequently, the sensitivity of brane inflation to the height and width of the steps is increased by several orders of magnitude.

However, the appearance of the warp factor in the potential typically destroys the flatness of the potential, so some fine-tuning is required. Here, we shall simply assume slow-roll with steps in the small field case.

2. Properties of steps in the infrared Dirac-Born-Infeld (IR DBI) model. In the UV DBI model, $D3$ -branes move down the throat at relativistic speed [12, 30]. In terms of known brane inflation scenarios, this model produces too large a non-Gaussianity to satisfy the current observational bound [31, 32, 33, 34] and inconsistent probe brane backreactions [35]. In the IR DBI model, inflation happens when $D3$ -branes are moving relativistically out of a throat [13, 36]. Recent analysis [35] shows that the IR DBI brane inflationary scenario fits the CMBR data quite well, comparable to a good slow-roll inflationary model. However, it has a regional large running of n_s : $-0.046 \lesssim dn_s/d \ln k \lesssim -0.01$ at $0.02/\text{Mpc}$ due to a stringy phase transition in primordial fluctuations. The spectral index has a red tilt $n_s \sim 0.94$ at $k \sim 0.02/\text{Mpc}$, and transitions to blue at larger scales. It also predicts a large distinct non-Gaussianity due to the DBI effect, which should be observable by PLANCK. So

we see that such IR DBI models of brane inflation can fit the present cosmological data and have distinctive stringy predictions different from slow-roll. In this DBI scenario, steps appear in the warp factor. The feature appearing in the power spectrum has different properties from that in the slow-roll case. For example, we can choose the phenomenological parameters that give reasonable fit to the glitch around $l \sim 20$, but given the extra parameters that are added, the improvement in χ^2 is not significant. We will explain why, in general, the glitches caused by the warp factor steps in IR DBI model is much smaller than the glitches in slow-roll inflation, while the associated non-Gaussianity signal can be very large. In this model, the non-Gaussianity should come from a combination of DBI relativistic roll effect together with the step effect, which can be large and is very distinctive.

As we shall see, some of the predictions are rather sensitive to the details, while others are robust, for example, that there are a number of steps, with their spacing $\Delta \ln \phi \propto \Delta \phi \propto \Delta \ln l$ roughly equal.

In the IR DBI model with steps, CMBR data can provide the following data points: n_s , $dn_s/d \ln k$, and DBI non-Gaussianity, which may be crudely quantified into four data points (the magnitude as measured by f_{NL} , two data points from the shape of the bi-spectrum, and another for its running¹). So the IR DBI scenario alone may confront CMBR via six data points. Comparing to the slow-roll case, which so far confronts CMBR via only n_s , the test of IR DBI is clearly much more restrictive. Note that the number of microscopic parameters of the model is roughly five (depending on how one counts) in both brane inflationary scenarios. Now, let us include the steps. Each step will provide three data points: its position, height and width, in addition to the non-Gaussianity associated with the step. The number of microscopic parameters of the model will increase by at least three. If we see more than one step in the CMBR, the test of the underlying superstring theory will be very stringent. In fact, we can learn a lot about the flux compactification of our universe in superstring theory. Of course, one may add the cosmic string prediction into the list to further test the scenarios.

We should mention that, broadly speaking, there are two classes of inflationary scenarios in string theory, depending on whether the inflaton is an open string mode (brane inflation) or a closed string mode (moduli inflation)². Moduli inflation can reproduce usual slow-roll inflation, but so far no distinct stringy signature has been identified. Obviously it is important to continue the search for distinct stringy signatures in both brane inflation and moduli inflation.

This paper is organized as follows. Section 2 reviews the setup of the geometry and the model. It also reviews $D3$ -brane potential where the step appears as a small correction. Section 3 presents general formalism on the power spectrum and bispectrum due to a sharp step. Section 4 discusses the step in the slow-roll brane inflation. Section 5 considers a

¹This accounting is clearly an oversimplification, since the bi-spectrum is a function. Furthermore, the 4 point-correlation (tri-spectrum) has also been calculated [37], which may be measured and tested.

²In brane inflation, inflatons are positions of branes, which are vacuum expectations of light open string modes. However, the inflaton potential can still be described by closed string interactions, perturbative, collective and/or otherwise.

step in the IR DBI model. We perform qualitative analyses of the step features in IR DBI inflation followed by numerical analyses. The comparison to WMAP data around $l \sim 20$ is also performed. To be more general, Sec. 3, 4 and 5 are written in a way that the main analyses apply to general sharp features, such as steps. The duality cascade steps reviewed in Sec. 2 is used as an example to give a more restrictive set of predictions. As we emphasized, some details of the steps such as the width, depth and forms may vary from example to example. In Section 6 we make some remarks on some broader aspects of brane inflation. A number of details are contained in the appendices.

2. The Model

First it is useful to define a basis of coordinates and a metric. The ten dimensional metric which describes the throat is that of $AdS_5 \times X_5$, where X_5 has the $T^{1,1}$ geometry in the UV region. Including the expansion of the universe, the metric has the form

$$ds^2 = h^2(r)(-dt^2 + a(t)^2 d\mathbf{x}^2) + h^{-2}(r)(dr^2 + r^2 ds_{X_5}^2), \quad (2.1)$$

Far away from the bottom of the throat, $ds_{X_5} = ds_{T^{1,1}}^2$ is the metric that describes a base of the conifold $T^{1,1}$ which is an S^3 fibered over S^2 . Here $h(r)$ is the warp factor, that is, a generic mass $m \rightarrow mh(r)$ in the presence of $h(r)$.

The inflaton ϕ is related to the position of n_B 4-dimensional space-time filling $D3$ -branes. In IR DBI inflation, they are moving out of the B throat into the bulk and then falling into the A throat. Inflation takes place while the branes are moving out of the B throat. In UV DBI inflation or the KKLMMT scenario, inflation takes place when they are moving down the A throat. Specifically, we use a single coordinate to describe collectively the motion of the branes,

$$\phi \equiv \sqrt{n_B T_3} r. \quad (2.2)$$

The edge of the throat is identified with $\phi_R \equiv \sqrt{n_B T_3} R$, with

$$R^4 = \frac{27}{4} \pi g_s N \alpha'^2, \quad N = KM. \quad (2.3)$$

In regions where several kinds of backreactions from the 4-dimensional expanding background [36, 38], the stringy effects [31, 36] and the probe-branes [12, 39] can be ignored, the following DBI-CS action describes the radial motion of the $D3$ branes,

$$S = \int d^4x \sqrt{-g} \left[-e^{-\Phi} T(\phi) \sqrt{1 - \frac{g^{\mu\nu} \partial_\mu \phi \partial_\nu \phi}{T(\phi)}} + T(\phi) - V(\phi) \right]. \quad (2.4)$$

The warped $D3$ brane tension $T(\phi)$ and the inflaton potential is given by

$$T(\phi) = n_B T_3 h^4(\phi), \quad (2.5)$$

$$V(\phi) = \frac{\beta}{2} H^2 \phi^2 + V_{D\bar{D}}(\phi), \quad (2.6)$$

$$V_{D\bar{D}}(\phi) = V_0 \left(1 - \frac{n_B V_0}{4\pi^2 v} \frac{1}{(\phi - \phi_A)^4} \right). \quad (2.7)$$

Here v is the volume ratio; one may take $v = 16/27$. For our purpose here, the Coulomb term is negligible so $V_{D\bar{D}}(\phi) = V_0 = 2n_A T_3 h^4(\phi_A)$ is the effective vacuum energy. We expect $|\beta| \sim 1$. Positive $\beta \gg 1$ for UV DBI model while negative $\beta \sim -1$ for IR DBI model. Slow-roll inflation requires $|\beta| \ll 1$.

It is convenient to introduce the inflationary parameter $\epsilon \equiv -\dot{H}/H^2$, so that

$$\frac{\ddot{a}}{a} = H^2(1 - \epsilon). \quad (2.8)$$

The universe is inflating when $\epsilon < 1$. In all the scenarios that we consider here, ϵ never grows to 1, so inflation ends by $D\bar{D}$ annihilation.

For simplicity, let us assume that the B throat is a KS throat. The warped factor for the B throat around the p_l^{th} duality transition (starting from the bottom of the throat) is simplified to (see Appendix A) [19]

$$h^4(r) \simeq \frac{r^4}{R_B^4} \frac{K}{p_l} (1 + \Delta), \quad \Delta = \sum_{p_i}^K \frac{3g_s M}{16\pi} \frac{1}{p^3} \left[1 + \tanh\left(\frac{r - r_p}{d_p}\right) \right], \quad (2.9)$$

where $h(r = R_B) \simeq 1$ at the edge of the throat. Here r_p is the positions of the steps, the initial $p_i \gg 1$ so that the warped factor formula is approximately good, and d_p controls the width of the step. The steps has a constant separation in $\ln r$, that is, $\ln r_{p+1} - \ln r_p \simeq 2\pi/3g_s M$. As one moves down the throat (r and p decreasing), note that the step in the warped factor $h^4(r)$ of the KS throat is going down. See Figure 1. This stepping down happens at each Seiberg duality transition. Together, they form a cascade [18]. For large K , one encounters $K - 1$ steps as one approaches the infrared. Note that we are ignoring smooth corrections to the shape of the warp factor even though they may be larger than the step size. This is a reasonable approximation since it is the sharp features that will show up as distinctive features in the CMBR.

Steps are a generic feature: consider another throat whose gauge dual has n_G gauge factors, with appropriate bi-fundamentals [20]. As the gauge coupling of the gauge factor with the fastest running towards large coupling in the infrared (decreasing r) gets strong, Seiberg duality transition applies. This happens for each gauge group factor sequentially until we reach the same structure as the original gauge model. Typically, it takes n_G/n_s number of transitions to complete this cycle, where n_s is a factor in n_G (the KS throat has $n_G = n_s = 2$ so each cycle has only 1 transition). Because of the jump in the corresponding anomalous mass dimension, steps in the warp factor are very generic. It is also likely that for another throat with a different geometry, some steps may show up with an opposite sign. To be general, we shall discuss each of these scenarios. If the throat has relatively few steps, or if the steps are well separated, the impact of individual step on CMBR may be observable. Otherwise, the steps may be too close for them to show up in the power spectrum.

In the original KS throat solution, they take the approximation where the dilaton is constant. Here the dilaton factor, $e^{-\Phi}$, runs in general and is ϕ dependent. However, for the IR DBI inflation model we discuss in this paper, most of the DBI e-folds are generated at the tip of the throat where $HR_B^2/N_e < r < HR_B^2$. At the same time, the brane moves

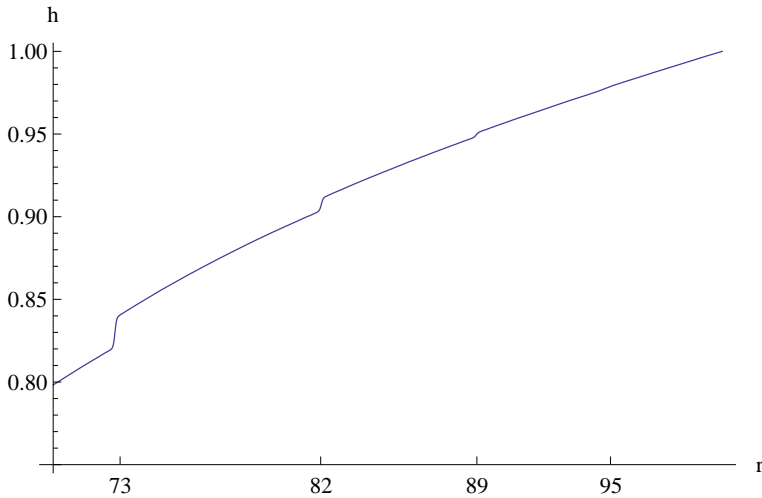


Figure 1: The warp factor $h(r)$ in the KS throat, including the steps. Here r is measured in $\sqrt{\alpha'}$ with $R_B \simeq 100$, $g_s = 2$, $M=20$, $K = 10$ and $N = 200$. The width $d = 10^{-3}$. In this figure, there are actually 4 steps, located at $r \simeq 73$, $r \simeq 82$, $r \simeq 89$ and $r \simeq 95$, although the step at $r \simeq 95$ is too small to show up. Here, the parameters (in particular, a large $g_s M$) are chosen so that at least 3 steps are big enough to show up in the figure. This leads to relatively large corrections to the positions of the steps. Other parameters should be used in more realistic situations and in comparison with data.

across roughly $g_s M$ steps [35]. The running of the dilaton can be ignored if $g_s M \ll p_l$, which is most easily satisfied with a small g_s . Furthermore, the WMAP data only covers a few e-folds, which corresponds to $3g_s M/N_e$ steps, so we only need $p_l \gtrsim g_s M$ to safely ignore the dilaton modification to the kinetic term. In this paper, when we discuss the IR DBI inflation, we always absorb e^Φ into g_s as a constant, so it will never appear explicitly in our analysis.

The energy density and pressure from the DBI action are given by

$$\rho = V(\phi) + T(\phi)(c_s^{-1} - 1), \quad p = -V(\phi) + T(\phi)(1 - c_s), \quad (2.10)$$

where the sound speed is defined as the inverse of the Lorentz factor γ ,

$$c_s = \gamma^{-1} = \sqrt{1 - \dot{\phi}^2/T}. \quad (2.11)$$

The background equation of motion is given by

$$V(\phi) + T(\phi)(c_s^{-1} - 1) = 3H^2, \quad (2.12)$$

$$\ddot{\phi} - \frac{3T'(\phi)}{2T(\phi)}\dot{\phi}^2 + 3Hc_s^2\dot{\phi} + T'(\phi) + c_s^3[V'(\phi) - T'(\phi)] = 0. \quad (2.13)$$

On the other hand, the running dilaton is more relevant for the UV DBI or the KKLMMT scenario, because here inflationary e-folds are generated by the $D3$ brane moving all the way from the UV to the IR end of the throat. For the KKLMMT scenario, we

expand the DBI action in the $\dot{\phi}^2 \ll T(\phi)$ limit, and get the slow-roll action,

$$S_{SR} = \int d^4x \sqrt{-g} \left[\frac{1}{2} e^{-\Phi} \dot{\phi}^2 - T(\phi)(e^{-\Phi} - 1) - V(\phi) \right]. \quad (2.14)$$

We see explicitly that the effective inflaton potential, $V_{\text{eff}}(\phi) = T(\phi)(e^{-\Phi} - 1) + V(\phi)$, now exhibits the step feature from $T(\phi)$. In the original KS solution, $e^{-\Phi} = 1$, and the steps in the warp factor do not affect the inflaton potential. The term $T(\phi)(e^{-\Phi} - 1)$ is generically bad for slow-roll inflation, however. Since $T(\phi) \sim \phi^4$, we have effectively introduced a quartic term in the potential. It is well known that a $\lambda\phi^4$ -type potential requires a trans-Planckian ϕ to generate inflation. However, in the KS throat (and other GKP type compactifications [10]), trans-Planckian ϕ is impossible [40, 32] and we have a strong bound on the largest inflaton field value,

$$\frac{\Delta\phi}{M_{\text{pl}}} \lesssim \frac{1}{\sqrt{KM}} \ll 1. \quad (2.15)$$

In order to get slow-roll inflation, the dominant term in the potential has to be the uplifting term from $\bar{D}3$ at the bottom of the throat, so we require

$$V_0 \gg T(\phi)(e^{-\Phi} - 1). \quad (2.16)$$

Since $V_0 \sim h^4(\phi_A) \ll T(\phi) \sim h^4(\phi)$, the above relation is true only when $e^{-\Phi} \approx 1$. Note that if V_0 dominates the inflaton potential, the step height in the inflaton potential is not given by Δ as defined in Eq.(2.9), but is suppressed by a factor $(e^{-\Phi} - 1)\phi^4/\phi_A^4 \ll 1$, i.e.

$$\frac{\Delta V}{V} = (e^{-\Phi} - 1) \frac{\phi^4}{\phi_A^4} \Delta. \quad (2.17)$$

So far, we have argued that even if the dilaton runs generically, slow-roll inflation can only occur within the region where $e^{-\Phi}$ stays close to 1. Thus when we discuss slow-roll scenario in this paper, we will ignore the $e^{-\Phi}$ modification to the kinetic term, and set $e^{-\Phi} \dot{\phi}^2 \approx \dot{\phi}^2$, but we keep the term $T(\phi)(e^{-\Phi} - 1)$ in the potential. This approximation should be pretty good, since $e^{-\Phi}$ only exhibits mild features like kinks, while $T(\phi)$ has sharp features like steps. When both of them are present, the sharp features in $T(\phi)$ definitely dominate.

3. The Power Spectrum and Bispectrum in General

The gauge invariant scalar perturbation $\zeta(\tau, \mathbf{k})$ can be decomposed into mode functions

$$\zeta(\tau, \mathbf{k}) = u(\tau, \mathbf{k})a(\mathbf{k}) + u^*(\tau, -\mathbf{k})a^\dagger(-\mathbf{k}). \quad (3.1)$$

The mode function $u_{\mathbf{k}}(\tau)$ is given by the equation of motion

$$v_k'' + \left(k^2 c_s^2 - \frac{z''}{z} \right) v_k = 0, \quad (3.2)$$

where

$$v_k \equiv z u_k, \quad z \equiv a\sqrt{2\epsilon}/c_s, \quad (3.3)$$

and prime denotes derivative with respect to the conformal time τ (defined as $dt \equiv a d\tau$). In the absence of any features in either potential or warp factor, the power spectrum is given by

$$P_{\mathcal{R}}(k) \equiv \frac{k^3}{2\pi^2} |u_{\mathbf{k}}|^2 \quad (3.4)$$

$$= \frac{H^2}{8\pi^2 M_{\text{pl}}^2 \epsilon c_s}, \quad (3.5)$$

where $u_{\mathbf{k}}$ is $u(\tau, \mathbf{k})$ evaluated after each mode crosses the horizon.

To study the effects of features, we define the inflationary parameters as below

$$\epsilon \equiv -\frac{\dot{H}}{H^2}, \quad \tilde{\eta} \equiv \frac{\dot{\epsilon}}{H\epsilon}, \quad s \equiv \frac{\dot{c}_s}{Hc_s}. \quad (3.6)$$

We can express z''/z exactly as,

$$\frac{z''}{z} = 2a^2 H^2 \left(1 - \frac{\epsilon}{2} + \frac{3\tilde{\eta}}{4} - \frac{3s}{2} - \frac{\epsilon\tilde{\eta}}{4} + \frac{\epsilon s}{2} + \frac{\tilde{\eta}^2}{8} - \frac{\tilde{\eta}s}{2} + \frac{s^2}{2} + \frac{\dot{\tilde{\eta}}}{4H} - \frac{\dot{s}}{2H} \right). \quad (3.7)$$

The z''/z encodes all the information from the inflationary background, and determines the evolution of $u(\tau, \mathbf{k})$. In the absence of sharp features, ϵ , η and s remains much smaller than 1, so $z''/z \sim 2a^2 H^2$. However, a sharp feature in the inflation potential or the warp factor will induce a sharp local change in ϵ , $\tilde{\eta}$ and s , and z''/z has a nontrivial behavior deviating strongly from $2a^2 H^2$ around the feature. In this paper, we have analyzed two cases. First, the slow roll brane inflation with a step feature in the inflaton potential $V(\phi)$. Due to the small field nature of brane inflation, ϵ is negligible, which greatly simplifies z''/z to (See Appendix B)

$$\frac{z''}{z} \approx 2a^2 H^2 \left(1 - \frac{V''(\phi)}{2H^2} \right) = 2a^2 H^2 \left(1 - \frac{3}{2} \frac{V''}{V} \right). \quad (3.8)$$

Second, the IR DBI brane inflation scenario with a sharp step appearing in the warp factor. In Section 5.2.2, we show that the sharp change of the sound speed is the major contribution to z''/z , and we have

$$\frac{z''}{z} \approx 2a^2 H^2 \left(1 - \frac{\dot{s}}{2H} \right) = 2a^2 H^2 \left(1 - c_s \epsilon \frac{T''}{T} \right), \quad (3.9)$$

where T is the warped brane tension defined in Eq.(2.5). To avoid confusion, we emphasize that the primes on z or u_k (functions of time) denote the derivative with respect to the conformal time τ , while the primes on T or V (functions of ϕ) denote the derivatives with respect to the field ϕ .

Among all the terms in the exact cubic action for the general single field inflation [41], the 3pt for sharp features receives dominant contribution from the term proportional to $\frac{d}{d\tau}(\frac{\tilde{\eta}}{c_s^2})$ in most interesting cases,

$$\begin{aligned} \langle \zeta^3 \rangle &= i \left(\prod_i u_{k_i}(\tau_{\text{end}}) \right) \int_{-\infty}^{\tau_{\text{end}}} d\tau a^2 \frac{\epsilon}{c_s^2} \frac{d}{d\tau} \left(\frac{\tilde{\eta}}{c_s^2} \right) \left(u_{k_1}^*(\tau) u_{k_2}^*(\tau) \frac{d}{d\tau} u_{k_3}^*(\tau) + \text{perm} \right) \\ &\times (2\pi)^3 \delta^3 \left(\sum_i \mathbf{k}_i \right) + \text{c.c.} . \end{aligned} \quad (3.10)$$

The reason is a generalization of that in Ref. [28]. As we will show, ϵ and c_s do not change much due to approximate energy conservation relations; but they change in a very short period of time, boosting $\dot{\epsilon}$ or \dot{c}_s by several orders of magnitude.

4. Steps in Slow-Roll Brane Inflation

In the slow-roll scenario, let us assume that inflation takes place as the brane moves down the throat. Since the dilaton runs, the slow-roll potential is given by

$$V_{SR}(\phi) = V(\phi) + T(\phi)(e^{-\Phi(\phi)} - 1) . \quad (4.1)$$

Here, the second term in the potential does not vanish, so the step in $T(\phi)$ shows up in the potential. Again, we may consider both step up and step down cases.

Before we proceed, we mention two other possibilities that will not be studied in more detail in this paper. Suppose the warp factor steps down as r increases. As the inflaton moves down the throat, it encounters such steps. If the height of any particular step is too big, then the inflaton cannot overcome it so its classical motion towards the bottom of the throat is stopped. Let us say this happens at $r = r_p$. It can still move along the $S^3 \times S^2$ angular directions. In a realistic model, the $S^3 \times S^2$ symmetry is slightly broken so the inflaton would move along the steepest angular direction, until it reaches the lowest point at this radius r_p . If the step there is lessened so that the inflaton can roll over it, the inflaton can continue to roll down along r until it reaches the next step. This process can repeat some number of times. As a result, the inflaton path is substantially longer than just moving down along r . Effectively, this may substantially extend the field range and enough e-folds of inflation is much more likely.

Another possibility is that the brane can tunnel over the step barrier. Recent analysis of the tunneling of branes suggests that, under the right condition, the brane may tunnel very easily across a potential barrier that is not particularly small [42]. If this is the case, then the brane may roll along some angular direction until it reaches such a position and tunnel right over the potential barrier there. It can then roll down along r until it reaches the next step. Again, this process can repeat any number of times, as a result, the inflaton path is again substantially longer than just moving down along r , allowing the generation of many e-folds.

In the following, we consider the scenarios where the inflaton can roll over many steps in the potential.

4.1 The Position of the Steps

The duality cascade predicts more than one step, so it is interesting to ask where the steps are. Assume there is a step at the $l \simeq 20$ in the CMBR, which may be checked with a non-Gaussianity measurement. Let us further assume that there is another step at $l \simeq 2$, (the significance of the signal at $l = 2$ in power spectrum is much smaller than that in $l \simeq 20$ due to the large cosmic variance, so we assume this mainly for the purpose of illustration). We now show that the location of all the steps in the duality cascade can be determined by given the locations of two such adjacent steps.

Using $l \sim 10^4(k/\text{Mpc}^{-1})$, we find

$$-dN_e \simeq d \ln k \simeq d \ln l \simeq H dt \simeq \frac{H}{\dot{\phi}} d\phi, \quad (4.2)$$

Since both H and $\dot{\phi}$ are slowly varying during inflation, we have

$$d \ln l \propto d\phi. \quad (4.3)$$

Suppose ϕ is decreasing (going down a throat), also suppose that the step at $l = 2$ is at ϕ_{m_0} and that at $l = 20$ is at ϕ_{m_0+1} , we have

$$\frac{\phi_{m_0}}{\phi_{m_0+1}} \simeq \frac{\phi_{m_0+1}}{\phi_{m_0+2}} \simeq \dots \simeq e^{2\pi/3g_s M}. \quad (4.4)$$

For large $g_s M$, this ratio is close to unity, $e^{2\pi/3g_s M} \simeq 1 + \delta$, so $\phi_{m_0} - \phi_{m_0+1} \simeq \phi_{m_0+1} - \phi_{m_0+2} \simeq \phi_{m_0+1} \delta$. Due to (4.3), equal spacing in ϕ implies equal spacing in $\ln l$. So we find that the next two steps are at around $l \simeq 200$ and $l \simeq 2000$ respectively. In addition, the effect of the step at multiple moment l should span over Δl multiple moments with $\Delta l \propto l$.

4.2 The Power Spectrum

In the slow-roll scenario without features, we have the attractor solution, in units of M_P ,

$$H^2 = V(\phi)/3, \quad 3H\dot{\phi} = -V'(\phi), \quad (4.5)$$

where $'$ is derivative with respect to the inflaton $\phi(t)$ and dot is derivative with respect to time. Here,

$$\epsilon = -\frac{\dot{H}}{H^2} = 2 \left(\frac{H'}{H} \right)^2 = \frac{1}{2} \left(\frac{V'}{V} \right)^2 = \epsilon_{SR}. \quad (4.6)$$

It is convenient to introduce another inflationary parameter

$$\tilde{\eta} = \dot{\epsilon}/H\epsilon = -2\eta_{SR} + 4\epsilon_{SR} \quad (4.7)$$

where the usual slow-roll version is given by

$$\eta_{SR} = \frac{V''}{V}. \quad (4.8)$$

This yields $n_s - 1 = -\tilde{\eta} - 2\epsilon = 2\eta_{SR} - 6\epsilon_{SR}$. We emphasize that the above relations between ϵ , $\tilde{\eta}$ and ϵ_{SR} , η_{SR} only hold for the attractor solution in absence of sharp features. We will use the parameters ϵ and $\tilde{\eta}$ in our analyses for the sharp feature case.

To see the full details of the effect of a step in potential, numerical calculation is necessary. However, the qualitative behavior can be estimated as follows. The step in the potential is typically characterized by two numbers: the depth which we describe as the ratio $\Delta V/V \approx 2c$, and the width $\Delta\phi = 2d$ in unit of Planck mass. We can divide the motion of inflaton into two parts: acceleration and relaxation. First, the inflaton, originally moving in its attractor solution, momentarily gets accelerated by the step. The potential energy ΔV gets converted to kinetic energy. Then after the inflaton moves across the step,

it starts to relax back to its attractor solution under $\ddot{\phi} + 3H\dot{\phi} \approx 0$, where the Hubble friction term dominates over the potential.

We first look at the power spectrum. The inflaton velocity in the original attractor solution is given by $|\dot{\phi}_{attr}| \approx |V'|/3H \approx \sqrt{\epsilon V/3}$. After the acceleration of the step, $\dot{\phi} \approx \sqrt{V(3c + \epsilon/3)}$. (It turns out that the best fit data give comparable $3c$ and $\epsilon/3$, so for the purpose of order-of-magnitude estimate we later will also approximate $\dot{\phi}$ to be $\sqrt{3cV}$.) A useful formula to understand the dip of the glitch in the power spectrum caused by the step is $P_{\mathcal{R}} = H^2/(4\pi^2\dot{\phi}^2)$. The acceleration of inflaton does not change the H so it reduces the $P_{\mathcal{R}}$. The ratio of $P_{\mathcal{R}}$ between the initial value and the value at the first dip is related to the corresponding ratio of $\dot{\phi}$, which is $\sqrt{1 + 9c/\epsilon}$. For the large field quadratic inflation, Ref. [26, 27] give the best-fit data, $c = 0.0018$, $\epsilon = 0.009$. As we will see later, the values of c and ϵ will be rather model-dependent. However the discussion in this paragraph shows that their ratio should be fixed for a specific observed feature,

$$\frac{c}{\epsilon} \approx 0.2 . \quad (4.9)$$

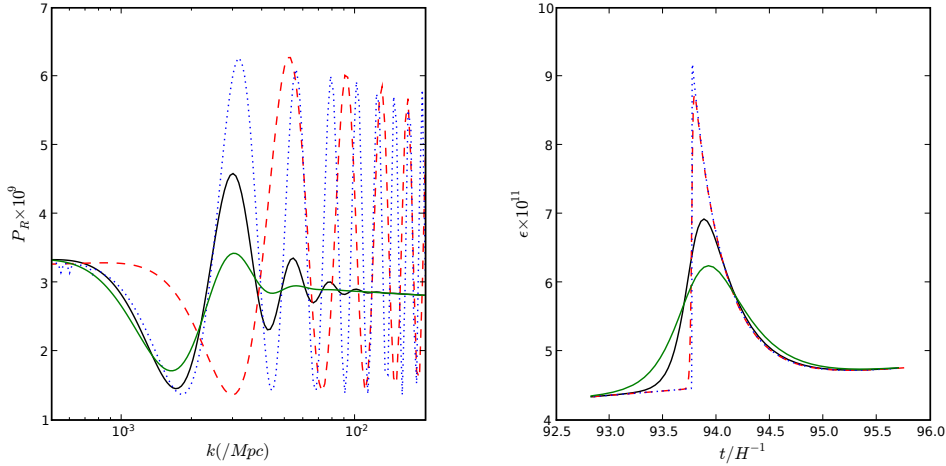


Figure 2: In the small field case, we show how the step in the inflaton potential changes the power spectrum. We show the power spectrum in the left panel and the behavior of ϵ around the step in the right panel. For illustration, we use the KKLMNT scenario with only the Coulomb potential. We choose the background flux $N = 2000$, so $\Delta\phi/M_{\text{pl}} \lesssim 0.01$. The inflation scale $V_0 \sim 10^{-17} M_{\text{pl}}^4$. ϵ is tiny, typically $\epsilon \sim 10^{-11}$ as shown in the right panel. We introduce a step with $c = 8 \times 10^{-12}$ and calculate the power spectrum for four different values of d : (1) $d = 3 \times 10^{-6} M_{\text{pl}}$, green solid line. (2) $d = 1.7 \times 10^{-6} M_{\text{pl}}$, black solid line. (3) $d = 1.7 \times 10^{-7} M_{\text{pl}}$, red dashed line. (4) $d = 1.7 \times 10^{-8} M_{\text{pl}}$, blue dotted line. Note that the dip in the power spectrum depends weakly on d . In case (1) and (2), $\Delta\epsilon$ has not saturated the bound Eq. 4.10, so decreasing d will enhance the bump in $P_{\mathcal{R}}$ significantly. In case (3) and (4), where $\Delta\epsilon$ is maximized, the bump in $P_{\mathcal{R}}$ does not depend sensitively on d , but the range of the oscillations in k -space does. The black solid line is close to the best fit power spectrum given in Ref. [26, 27].

Although the above discussion indicates that the depth of the dip is relatively independent of d , the peak of the first bump is. When the inflaton moves across the step, energy conservation requires that $\frac{1}{2}\Delta\dot{\phi}^2 \leq \Delta V$, with the bound saturated when the Hubble friction is negligible. This will result in an upper bound in the change of ϵ

$$\Delta\epsilon \approx \Delta V/H^2 \lesssim 5c. \quad (4.10)$$

We expect that the effect of decreasing d will first enhance the bump, since smaller d leads to more deviation from the attractor (larger $\Delta\epsilon$), and will enhance the bumps in $P_{\mathcal{R}}$ during the relaxation period. However, as long as $\Delta\epsilon$ saturates the upper bound (when d is small enough to ignore the Hubble friction), further decreasing d will not affect the bumps in $P_{\mathcal{R}}$ any more, since the relaxation period essentially starts with the same $\dot{\phi}$ no matter how small d is. So we expect the bump to depend sensitively on d if moving across the step takes $\mathcal{O}(1)$ e-folds, and it becomes relatively insensitive to d when the step is so sharp that moving across it takes only $\ll 1$ e-folds. In the latter situation, reducing d will only increase the extension of the oscillations in $P_{\mathcal{R}}$,

$$\Delta k \sim \sqrt{\frac{z''}{z}} \sim k_0 \frac{\sqrt{c}}{d}, \quad (4.11)$$

where k_0 is the starting point of the feature, and (3.8) is used.

Ref. [26, 27] fit the $l \sim 20$ feature in the WMAP data introducing a step feature in the large field slow-roll model and gives the best fit power spectrum. Here we have numerically reproduced a similar power spectrum for the small field case. We are not performing a complete data analysis to find the best fit model here, our major emphasis is to show how the width d comes into play. Fig. 2 shows the power spectrum and ϵ for four different values of d . The black solid line represents the power spectrum close to the best fit model given in Ref. [26, 27], with $c = 8 \times 10^{-12}$, we find that $d = 1.7 \times 10^{-6} M_{\text{pl}}$.

4.3 Non-Gaussianities

Now let us look at the bispectrum. For slow-roll inflation, the 3-point function of the scalar perturbation $\zeta(\tau_{\text{end}}, \mathbf{k})$ includes terms proportional to ϵ^2 , ϵ^3 , and $\epsilon\tilde{\eta}'$ [43]. For the slow-roll potential without any features, the first terms dominate. Comparing to WMAP's ansatz, it gives the non-Gaussianities estimator $f_{NL} = \mathcal{O}(\epsilon)$.

In the presence of sharp features, from (4.10) we see that ϵ still remains small, $\lesssim \mathcal{O}(0.01)$. But $\tilde{\eta}'$ can be much larger. Therefore, the leading three-point correlation function is given by the term proportional to $\epsilon\tilde{\eta}'$ [28],

$$\begin{aligned} & \langle \zeta(\tau_{\text{end}}, \mathbf{k}_1) \zeta(\tau_{\text{end}}, \mathbf{k}_2) \zeta(\tau_{\text{end}}, \mathbf{k}_3) \rangle \\ &= i \left(\prod_i u_{k_i}(\tau_{\text{end}}) \right) \int_{-\infty}^{\tau_{\text{end}}} d\tau a^2 \epsilon \tilde{\eta}' \left(u_{k_1}^*(\tau) u_{k_2}^*(\tau) \frac{d}{d\tau} u_{k_3}^*(\tau) + \text{perm} \right) \\ & \times (2\pi)^3 \delta^3(\sum_i \mathbf{k}_i) + \text{c.c.}, \end{aligned} \quad (4.12)$$

where the ‘‘perm’’ stands for two other terms that are symmetric under permutations of the indices 1, 2 and 3. The details of such an integration are quite complicated. Nonetheless we

can estimate the order of magnitude of the non-Gaussianity estimator f_{NL} by comparing it to the slow-roll case. The most important difference is that here we replace a factor of ϵ by $\tilde{\eta}'$, and also $\tilde{\eta}'$ only gets large momentarily. Hence we estimate $f_{NL}^{\text{feature}} = \mathcal{O}(\tilde{\eta}' \Delta\tau) = \mathcal{O}(\Delta\tilde{\eta})$, where $\Delta\tau$ is the conformal time that the inflaton spends crossing the step.

To estimate the level of these non-Gaussianities, we now give a qualitative estimate for $\tilde{\eta}'$ [28]. During the acceleration period, the ϵ is increased by

$$\Delta\epsilon \approx \Delta V/H^2 \approx 5c . \quad (4.13)$$

The duration of this period is

$$\Delta t_{\text{accel}} \approx \Delta\phi/\dot{\phi} \approx d/\sqrt{cV} , \quad (4.14)$$

where we used $\dot{\phi}$ estimated in Sec. 4.2. These can be further used to estimate

$$\Delta\tilde{\eta} \approx \tilde{\eta} = \frac{\dot{\epsilon}}{H\epsilon} \approx \frac{7c^{3/2}}{d\epsilon} , \quad (4.15)$$

The time scale for the relaxation period is of order H^{-1} , during which $\tilde{\eta}$ is $\mathcal{O}(1)$ and $\dot{\tilde{\eta}}$ are of order $\mathcal{O}(H)$.

We sum over the contributions from both the acceleration and relaxation periods. The former gives $f_{NL}^{\text{accel}} \approx 7c^{3/2}/(d\epsilon)$, the latter gives $f_{NL}^{\text{relax}} = \mathcal{O}(1)$. So for most interesting cases where non-Gaussianities are large enough to be observed, it can be estimated by the first contribution,

$$f_{NL}^{\text{feature}} \sim \frac{7c^{3/2}}{d\epsilon} . \quad (4.16)$$

We note that this is only a crude order of magnitude estimation on the amplitude of this non-Gaussianity, since the integration (4.12) also involve mode functions u_k which will be modulated by the presence of the sharp feature, and the shape and running of such non-Gaussianities are very important. Details have to be done numerically, as in [28]. Qualitatively since we have argued in Sec. 4.2 that for a specific observed feature the c/ϵ is hold fixed model-independently, (4.16) implies that the value of d is very crucial to the level of the non-Gaussianities. There are two major constraints on d . First, in the power spectrum, as shown in Fig. 2 the bump in $P_{\mathcal{R}}$ may depend sensitively on d . Second, the range of oscillation in $P_{\mathcal{R}}(k)$ is also controlled by d . If d is too small, the oscillation in $P_{\mathcal{R}}(k)$ might spread over to the well measured first acoustic peak in WMAP C_l curve. Numerically, we have found that $\sqrt{c}/d \sim \mathcal{O}(1)$, consistent with (4.11), so the magnitude of (4.16) should be close to that in Ref. [28].

It is instructive to split this expression to $f_{NL}^{\text{feature}} \sim 7c/\epsilon \cdot \sqrt{c}/d$. The first factor is determined by the amplitude of the glitch from (4.9), while the second factor is the extension of the glitch from (4.11). Note both are in the k -space not the CMB multipole l -space. Therefore in principle a sharp feature can also appear only in the 3-point function. This is clear from our estimation (4.9) and (4.16), where one can reduce c/ϵ while increase $c^{3/2}/(d\epsilon)$.

Our analyses so far do not depend on the whether the inflation is caused by large field or small field, but when it comes to the quantitative analyses the differences are

interesting. For large field inflation $\epsilon \sim \eta$ while for small field inflation $\epsilon \ll \eta$. For example, previous numerical works focus on the large field quadratic potential, and give the best fit $\Delta V/V \sim c \sim 0.2\epsilon \sim \mathcal{O}(10^{-3})$. Brane inflation is a small field inflation [40] and ϵ is much smaller, $\epsilon \sim \mathcal{O}(10^{-6})$ or even $\mathcal{O}(10^{-12})$. Similarly the field range d (in units of M_{pl}) is also much smaller. So brane inflation is sensitive to very tiny steps present in the potential. This can be potentially used as a sensitive probe to the fundamental theory.

5. Steps in IR DBI Inflation

The DBI-CS action is Eq.(2.4) with $V(\phi) = V_0 - \frac{1}{2}m^2\phi^2$. The branes start from the tip of the throat and end at the UV end of the throat $\phi_{\text{end}} = R_B\sqrt{n_B T_3} = \sqrt{\lambda_B}/R_B$. After that, branes will quickly find antibranes and annihilate.

In the relativistic (DBI) regime with $t \ll -H^{-1}$, the attractor solution is

$$\phi \simeq -\frac{\sqrt{\lambda_B}}{t} \left(1 - \frac{9}{2\beta^2 H^2 t^2} \right), \quad \gamma \simeq \frac{\beta H}{3} |t|. \quad (5.1)$$

This zero mode evolution relies on the background warped geometry, so it is reliable in regions where the back-reaction deformation from Hubble expansion is small [36, 38]. This still leaves at least two interesting regions for primordial fluctuations: the field theoretic region (corresponding to smaller N_e and shorter scales) and the stringy region (corresponding to bigger N_e and larger scales). The spectral index transitions from red to blue [36, 31]. Detailed estimates can be found in Ref. [35].

We now consider the effects of sharp features in the warped geometry on this IR DBI model. The duality cascade will leave sharp features on the warp factor $T(\phi)$ but not the inflaton potential $V(\phi)$. Since the WMAP window spans a few e-folds, corresponding to branes rolling across $\Delta l \approx 3g_s M/N_e^{\text{DBI}}$ duality cascades in a Klebanov-Strassler throat. In this paper we will mainly treat the steps as individual sharp features, namely they are well separated in terms of e-folds and sufficiently sharp to generate observational signature individually. For this purpose, we would like to consider the situation where

$$g_s M \lesssim N_e^{\text{DBI}}. \quad (5.2)$$

In the multi-throat brane inflation scenario, the number of inflaton branes generated in B-throat is roughly determined by the flux number M . Since the number of inflaton branes is constrained to be around $10^4 \sim 10^5$ [35], the condition (5.2) implies a small $g_s \lesssim 10^{-3}$.

It is also very natural that g_s takes value larger than 10^{-3} . In this case, the branes come across many steps within a single e-fold. We will discuss this case in Sec. 5.5.

5.1 The Properties of the Steps

Here we like to make a crude estimate on the positions, fractional heights and widths of the steps, along the line of Sec. 4.1 but with more detailed numbers. The input is the position, fractional height and width of the step at $l \sim 20$ as well as the position of the assumed

step at $l \sim 2$. Let $r = r_0 \simeq R_B$ be the edge of the throat and $r = r_b$ at the bottom of the throat. They are related by the warp factor $h(\phi_b) = h_B$,

$$r_b \sim r_0 h_B \sim r_0 \exp\left(-\frac{2\pi K}{3g_s M}\right). \quad (5.3)$$

We are interested at regions where $r_b \ll r \ll r_0$. Thus, given r_0 or r_b , we can determine all the other transition values r_p . Here p measures (starting at the bottom) the step in the duality cascade. In the large $K \gg p \gg 1$ limit, the correction is small, so we treat the steps as perturbations. The sharpness of the steps are controlled by the coefficient d_p . A step becomes infinitely sharp as $d_p \rightarrow 0$. We shall leave d_p as free parameters. Note we can introduce similar spreads to the running of the dilaton.

The position ϕ_p of the steps can be computed. The steps are at $\phi = \phi_p$, where

$$\ln \frac{\phi_p}{\phi_b} \simeq \frac{2\pi}{3g_s M} \left(p - \frac{1}{2p}\right) \sim \frac{2\pi p}{3g_s M}. \quad (5.4)$$

Same as Eq.(4.2) in the slow-roll case, we have

$$-dN_e \simeq d \ln k \simeq d \ln l \simeq H dt. \quad (5.5)$$

Suppose the p th step is at l_p (or ϕ_p), because $\phi \simeq -\sqrt{\lambda_B}/t$, we get

$$\frac{\phi_p}{\phi_{p-1}} \simeq \frac{t_{p-1}}{t_p} \simeq \frac{N_0 - \ln l_{p-1}}{N_0 - \ln l_p}, \quad (5.6)$$

where we have used the fact that H is approximately a constant, and N_0 is the number of e-folds (at the largest CMBR scale) to the end of DBI inflation, for example $N_0 \approx 38$ [35]. On the other hand, duality cascade relates the position of the adjacent steps

$$\frac{\phi_p}{\phi_{p-1}} = \exp\left(\frac{2\pi}{3g_s M}\right). \quad (5.7)$$

Suppose the feature at $l_{p_i+1} \sim 20$ is due to such a step, and suppose the feature at $l_{p_i} \sim 2$ is also due to a step (not just cosmic variance). That is, p_i labels the initial or the first observable step. Then, taking $N_0 = 38$, we see that the next 2 steps should be at

$$l_{p_i+2} \sim 170 \quad l_{p_i+3} \sim 1300. \quad (5.8)$$

We also get a constraints on the microscopic parameters

$$g_s M \approx 33. \quad (5.9)$$

Now we estimate the value of p_i by looking at the dip in the CMB power spectrum at $l \sim 20$. The power spectrum is

$$P_{\mathcal{R}}(k) = \frac{H^4}{4\pi^2 \dot{\phi}^2}. \quad (5.10)$$

In IR DBI inflation, the Hubble scale is dominated by the constant $\sqrt{V_0}$, so it does not change across a step in the warp factor. However, since $\dot{\phi}$ closely tracks the speed limit

$\dot{\phi}^2 \sim h^4(\phi)$, it is most sensitive to the step in the warp factor. $\dot{\phi}^2$ increasing by a factor of $(1 + 2b)$ across a step decreases $P_{\mathcal{R}}$ by a factor of $(1 + 2b)$. The CMB data shows that around $l \sim 20$, there is a dip in the power spectrum by about 20% in k -space, which gives $2b \sim 0.2$. Using (2.9), we have

$$\left(\frac{3g_s M}{8\pi}\right) \frac{1}{(p_i + 1)^3} \sim 0.2 . \quad (5.11)$$

Given that $g_s M \approx 33$ to fit the spacing of the steps, we immediately get

$$p_i = 2 . \quad (5.12)$$

With input of 4 quantities : the position $l \sim 20$, the fractional height (size) $\Delta T/T \simeq 0.2$ and the width $\Delta l_p \sim 5$ of the 2nd step as well as the position (at $l \sim 2$) of the first step, we can use $\Delta l \propto l$ and $\Delta T/T \propto p^{-3}$ to get a complete set of predictions:

p	l	$\Delta T/T$	Δl_p
2	~ 2	~ 0.7	~ 1
3	~ 20	0.2	~ 5
4	~ 170	~ 0.08	~ 40
5	~ 1300	~ 0.04	~ 260

Note that $\Delta T/T \sim 0.7$ and $\Delta T/T = 0.2$ for the first two steps are probably too big to be treated as a perturbation. We shall take this to mean that the size of the first step can be very big.

We should point out that the warp factor Eq.(2.9) is a good approximation only when $p \gg 1$. This condition is also necessary to ignore the running of the dilaton. So $p = 3$ is already too small. Moreover, as we will see in Sec. 5.4, the glitch in the power spectrum around $l \sim 20$ may be too large to be explained by a step feature in the warp factor due to the duality cascades.

5.2 Qualitative Analyses around a Single Step

We consider a sharp step in the warped geometry $T(r)$. We parametrize the size of the step as $2b \equiv \Delta T/T$ and the width as $\Delta\phi \equiv 2d$. We use the tanh function interpolation between the two sides of the step, i.e.

$$T(r) \equiv T_3 \frac{r^4}{R^4} \left[1 + b \tanh\left(\frac{r - r_s}{d}\right) \right] . \quad (5.13)$$

5.2.1 The Evolution of the Sound Speed

We use the case of positive b to illustrate the evolution of the sound speed, the formulae are the same for negative b . The direction of the step is such that, for positive b , T steps up as r increases, i.e. the warp factor $h \propto T^{1/4}$ (or the speed-limit h^2) increases as r increases.

The first stage is when branes move across the step, where the speed-limit increases suddenly. Since the time that the branes spend to across the step is very short comparing to the Hubble time (see Appendix C), during which we can ignore the Hubble expansion

and the acceleration from the potential. So across the step, the behavior of the branes is approximated by the Lagrangian $L = -T(r)\sqrt{1 - \dot{\phi}^2/T(r)}$. The corresponding energy $T\gamma = \text{const}$, where $\gamma = 1/c_s = (1 - \dot{\phi}^2/T)^{-1/2}$. Hence a sharp change in T results in a sharp change in c_s , and both changes are small,

$$\frac{\Delta c_s}{c_s} = \frac{\Delta T}{T} = 2b . \quad (5.14)$$

A small change in c_s also means that the velocity of the branes will closely track the change of the speed-limit in step.

The second stage is at the end of the step, where the previous change in c_s results in a deviation from the attractor solution. To see this, we note that in IR DBI inflation, the attractor solutions have $\gamma \approx \beta N_{e\text{DBI}}/3$ and $N_{e\text{DBI}} \approx HR/h$, so $c_s \approx 3h/\beta HR$. A fractional change in the warp factor $h = r/R$ means $\Delta R/R = -b/2$, which implies that the attractor solution has a fractional change

$$\frac{\Delta c_s}{c_s} = b . \quad (5.15)$$

So the increase in c_s due to the first stage (5.14) over-shoots the new attractor solution, the branes will have to quickly relax to the new attractor solution. The Hubble expansion plays an important role here, so the energy $T\gamma$ is no longer conserved.

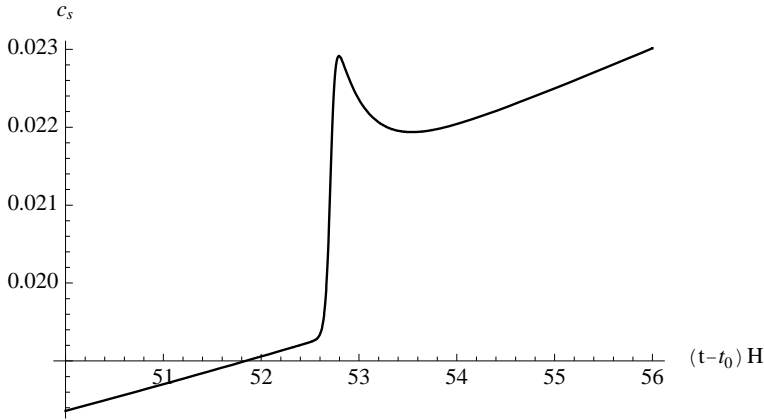


Figure 3: Evolution of c_s . Parameters are $b = 0.1$, step width $\Delta N_e = 0.05$, $\beta = 3$, $g_s m_s^{-4} = 10^{39}$, $N_B = 10^9$, $n_B = 10^4$, $n_A h_A^4 = 16$.

In summary, the behavior of c_s can be approximated by two step-functions side by side. In the first one, it jumps up from the original c_s to $c_s + 2bc_s$, during which the branes quickly fall down the step in warp geometry. The time scale is determined by d and is typically much smaller than $1/H$. The second one comes immediately afterwards, it jumps down from $c_s + 2bc_s$ to $c_s + bc_s$, during which the branes quickly approach the new attractor solution. The time scale is of order $\mathcal{O}(1/H)$. The width of the second step function is much larger than the first for narrower step (i.e. smaller d). Note that in both stages, the velocity of branes increases. This evolution is illustrated in Fig. 3.

Because the width of step is very small, such a small change of c_s happens in a short period. This gives rise to large $s \equiv \dot{c}_s/(c_s H)$ and \dot{s}/H . This turns out to be the primary sources to various observable signatures in power spectrum and non-Gaussianities.

5.2.2 The Power Spectrum

The power spectrum is determined by the mode equation Eq.(3.2). We now estimate various parameters in Eq. (3.7) in terms of the size, b , and width, d , of the step feature in the warp factor. It is convenient to write d in terms of the e-fold that the brane spends moving across it,

$$\Delta N_e \equiv H \Delta t \approx H \frac{d}{\dot{\phi}} = \frac{d}{\sqrt{2c_s \epsilon}} . \quad (5.16)$$

Note this is not the e-folds that the feature on CMB spans (denoted as Δl previously) which typically includes the oscillations and spreads much wider.

Using the continuity equation $\dot{\rho} = -3H(\rho + p)$, together with the energy density and pressure Eq.(2.10), we can solve for the evolution of s ,

$$s = \frac{\dot{c}_s}{H c_s} = 3(1 - c_s^2) + \frac{c_s \dot{V}}{TH} + \frac{\dot{T}}{TH}(1 - c_s) . \quad (5.17)$$

Here we can make more explicit the conditions under which the sharp features in warp factor dominate. On the right hand side of (5.17), to make the 3rd term larger than the first, i.e. to ignore the spatial expansion, we require $3 < \Delta T/(TH \Delta t) \approx 2b/\Delta N_e$; to ignore the 2nd term, i.e. the sharp features in potential, we require $c_s V' < T'$. Since the duality cascade leaves sharp steps on $T(\phi)$ but not $V(\phi)$, this condition is easily satisfied. Under these conditions, the last terms in the above equation dominates, so we can approximate

$$s \approx \frac{\dot{T}}{TH} \sim \frac{b}{d} \sqrt{2\epsilon c_s} \sim \mathcal{O}\left(\frac{b}{\Delta N_e}\right) . \quad (5.18)$$

This is consistent with (5.14).

Denote $X \equiv \dot{\phi}^2/2$, so $\epsilon = X/(M_{\text{pl}}^2 H^2 c_s)$ for DBI inflation. We get

$$\tilde{\eta} = \frac{\dot{\epsilon}}{H\epsilon} = \frac{\dot{X}}{HX} + 2\epsilon - s . \quad (5.19)$$

On the other hand, from the definition $c_s = \sqrt{1 - 2X/T(\phi)}$, we get

$$\frac{\dot{X}}{XH} = \frac{\dot{T}}{TH} - \frac{2c_s^2 s}{H(1 - c_s^2)} . \quad (5.20)$$

Plug (5.20) into (5.19), and use (5.17) to get rid of \dot{T}/TH , we have

$$\begin{aligned} \tilde{\eta} &= \frac{c_s}{1 + c_s} s - 3(1 + c_s) - \frac{\dot{V} c_s}{HT(1 - c_s)} + 2\epsilon \\ &\approx c_s s - \left(3 + \frac{\dot{V} c_s}{HT}\right) . \end{aligned} \quad (5.21)$$

Except for the first term, the r.h.s. of this expression is affected little, $\mathcal{O}(b)$, by the feature. We use (5.21) to further estimate $\dot{\eta}/H$. Keeping the time derivatives on c_s , $\dot{\phi}$ and T , while ignoring those on V' and H , we get

$$\frac{\dot{\eta}}{H} \approx \frac{3}{2}s + c_s s^2 + c_s \frac{\dot{s}}{H} . \quad (5.22)$$

We have used the fact that the brane always tracks the speed-limit,

$$\dot{\phi} \approx \sqrt{T(\phi)} , \quad \ddot{\phi} \approx \frac{1}{2} \frac{T'(\phi)}{T(\phi)} \dot{\phi}^2 , \quad (5.23)$$

since $c_s \ll 1$ even at the sharp feature as we know from Sec. 5.2.1. Eq. (5.18) is also used.

We further estimate \dot{s}/H ,

$$\begin{aligned} \frac{\dot{s}}{H} &= \left(\frac{T'(\phi)}{T(\phi)} \right)' \frac{\dot{\phi}^2}{H^2} + \frac{T'(\phi)}{T(\phi)} \left(\frac{1}{H} \frac{d}{dt} \frac{\dot{\phi}}{H} \right) \\ &\approx \left(\frac{T''}{T} - \frac{T'^2}{T^2} \right) \frac{\dot{\phi}^2}{H^2} + \frac{T'}{T} \frac{\ddot{\phi}}{H^2} . \end{aligned} \quad (5.24)$$

Using Eq.(5.23) to eliminate the $\ddot{\phi}$ in Eq.(5.24), we get

$$\frac{\dot{s}}{H} \approx 2c_s \epsilon \left(\frac{T''}{T} - \frac{1}{2} \frac{T'^2}{T^2} \right) \approx 2c_s \epsilon \left(\frac{T''}{T} \right) \sim b \frac{c_s \epsilon}{d^2} \sim \mathcal{O} \left(\frac{b}{\Delta N_e^2} \right) , \quad (5.25)$$

where we have dropped the term T'^2/T^2 , since $T''/T \gg T'^2/T^2$ as long as $b \ll 1$.

We now can compare the amplitudes of various terms. Because both b and ΔN_e are small, from (5.18) and (5.25), we have

$$\frac{\dot{s}}{H} \gg s, s^2 . \quad (5.26)$$

From (5.21) and (5.22),

$$s \gg \tilde{\eta} , \quad \frac{\dot{s}}{H} \gg \frac{\dot{\eta}}{H} . \quad (5.27)$$

So the only important contribution to z''/z is from \dot{s}/H , and we have

$$\frac{z''}{z} \approx 2a^2 H^2 \left(1 - \frac{\dot{s}}{2H} \right) \approx 2a^2 H^2 \left(1 - \frac{T''}{T} c_s \epsilon \right) . \quad (5.28)$$

If we take T to be the form Eq.(5.13), we can evaluate

$$\begin{aligned} \frac{z''}{z} &\approx 2a^2 H^2 \left[1 - b \frac{c_s \epsilon}{d^2} \operatorname{sech}^2 \left(\frac{\phi - \phi_s}{d} \right) \tanh \left(\frac{\phi - \phi_s}{d} \right) \right] \\ &\sim 2a^2 H^2 \left[1 - \frac{b}{\Delta N_e^2} \operatorname{sech}^2 \left(\frac{\phi - \phi_s}{d} \right) \tanh \left(\frac{\phi - \phi_s}{d} \right) \right] . \end{aligned} \quad (5.29)$$

The feature in z''/z is dictated by the $\operatorname{sech}^2 \tanh$ term, and will affect the evolution of certain perturbation modes v_k . As moving across the step only generates $\sim N_e^{DBI}/M$

e-folds (See Appendix C), typically $b/\Delta N_e^2 \gg 1$. The mode v_k will first see a dip in z''/z followed by a bump. Let us assume that the feature in z''/z shows up around conformal time τ_s , then modes with $c_s^2 k^2 \gg (z''/z)|_{\tau_s}$ or $c_s^2 k^2 \ll (z''/z)|_{\tau_s}$ will not be affected, because they are either oscillating well inside the sound horizon or have already crossed the sound horizon and got frozen. The major effect will be on the modes with $c_s^2 k^2 \sim (z''/z)|_{\tau_s}$. The range of k affected by the sharp feature is determined by $b/\Delta N_e^2$. If $P_{\mathcal{R}}$ starts seeing the feature at k_0 , the feature will disappear at

$$\Delta k \sim k_0 \sqrt{b}/\Delta N_e . \quad (5.30)$$

5.2.3 Non-Gaussianities

Although Ref. [41, 43, 44] are only interested in non-Gaussianities without sharp features, the cubic expansion of the perturbations is exact and does not rely on the assumption that various inflationary parameters ϵ , $\tilde{\eta}$ and s are small. For DBI inflation, among all the terms in Ref. [41], the leading term in the cubic action that is responsible for sharp features in non-Gaussianity is

$$\frac{a^3 \epsilon}{2c_s^2} \frac{d}{dt} \left(\frac{\tilde{\eta}}{c_s^2} \right) \zeta^2 \dot{\zeta} . \quad (5.31)$$

In the absence of sharp features, a term such as $(a^3 \epsilon/c_s^4) \zeta \dot{\zeta}^2$ contributes to the non-Gaussianity estimator $f_{NL} \sim 1/c_s^2$. Therefore as a rough estimate the term (5.31) contributes

$$f_{NL}^{\text{feature}} \sim \frac{d}{dt} \left(\frac{\tilde{\eta}}{c_s^2} \right) \Delta t \sim \Delta \left(\frac{\tilde{\eta}}{c_s^2} \right) . \quad (5.32)$$

The cases with large s are most interesting for non-Gaussianities. Using (5.21),

$$\tilde{\eta} \approx c_s s , \quad (5.33)$$

so

$$f_{NL}^{\text{feature}} \sim \frac{\Delta s}{c_s} \sim \frac{1}{c_s} \frac{b}{\Delta N_e} . \quad (5.34)$$

There is another term

$$-2 \frac{a\epsilon}{c_s^2} s \zeta (\partial \zeta)^2 \quad (5.35)$$

in the cubic action of Ref. [41] that contributes

$$f_{NL}^{\text{feature}} \supset \frac{s}{c_s^2} \Delta t H \sim \frac{\Delta c_s}{c_s^3} \sim \frac{b}{c_s^2} , \quad (5.36)$$

which is also possibly observable. The term (5.34) dominates for the most interesting cases.

The net observable effect will be a nearly-scale-invariant large non-Gaussianity of order $\mathcal{O}(1/c_s^2)$ plus the scale-dependent (oscillatory) modulation of order $\mathcal{O}(\Delta s/c_s)$. Similar to the slow-roll case, we can write $f_{NL}^{\text{feature}} \sim (\sqrt{b}/c_s)(\sqrt{b}/\Delta N_e)$. As we have shown, the

first factor determines the amplitude of the glitch in power spectrum through b , while the second factor determines the extension of its oscillations through (5.30). So there is a simple relation between the effects of sharp feature on the power spectrum and non-Gaussianity. For a same single visible glitch in power spectrum, the oscillatory amplitude of the bispectrum in DBI inflation is larger than that in slow-roll inflation mostly due to the factor of $1/c_s$ which can make f_{NL}^{feature} larger than $\mathcal{O}(10)$; while for glitches that have long oscillatory extension (which can also be made invisible in power spectrum with tiny b), the associated bispectrum can be very large with tiny ΔN_e . The estimates of b and ΔN_e in Appendix A and C suggest that the well-separated steps in the duality cascade tend to fall into the latter category. We will later see independent evidence from fitting the power spectrum glitch to WMAP CMBR data.

5.3 An Analytical Approximation for a Single Sharp Step

In this subsection, we give some analytical treatment of the effect of sharp feature on power spectrum. The full analyses rely on numerical calculations. Nonetheless we can see how several properties emerge and we summarize them in the end of this subsection.

In Section 5.2.1, we see that the sound speed undergoes two adjacent jumps. Here we simplify it by just considering the overall net effect, namely we approximate it by one step-function from c_s to $c_s = bc_s$. We approximate the transition to be infinitely sharp so that an analytical analysis is possible. As we showed, the width of the first step function can be made very small as we reduce d , while that of the second is much wider and of order $\mathcal{O}(1/H)$ model-independently. So this approximation is only qualitative.

We denote τ_0 to be the moment inflaton passes the feature, and look at the solutions of the equation of motion (3.2) at both sides of τ_0 . At $\tau = \tau_0^-$,

$$v_k = v_1|_{\tau_0^-} . \quad (5.37)$$

At $\tau = \tau_0^+$,

$$v_k = C_1 v_1|_{\tau_0^+} + C_2 v_2|_{\tau_0^+} . \quad (5.38)$$

Here we have denoted the two linearly independent solutions as

$$v_1 \equiv \frac{iaH}{\sqrt{2c_s^3 k^3}} (1 + ikc_s \tau) e^{-ikc_s \tau} , \quad (5.39)$$

$$v_2 \equiv \frac{iaH}{\sqrt{2c_s^3 k^3}} (1 - ikc_s \tau) e^{ikc_s \tau} . \quad (5.40)$$

For $\tau < \tau_0$ we only have v_1 because the vacuum is dominated by the Bunch-Davis vacuum.

These two solutions are matched according to the boundary conditions at τ_0 . These are contributed dominantly by the sharp change in z''/z in the last term of (3.2). From the previous subsection, we know that the change in $z \equiv a\sqrt{2\epsilon}/c_s$ is dominated by the change in c_s . As mentioned we approximate

$$c_s = c_s|_{\tau_0^-} + bc_s|_{\tau_0^-} \theta(\tau - \tau_0) , \quad (5.41)$$

where θ is the step-function. So

$$z = \begin{cases} z_-(\tau) , & \tau < \tau_0 , \\ z_0 - bz_0\theta(\tau - \tau_0) , & \tau = \tau_0 , \\ z_+(\tau) , & \tau > \tau_0 , \end{cases} \quad (5.42)$$

where $z_0 = z_-(\tau_0)$. Around τ_0 , we then have

$$v_k'' \approx \frac{z''}{z} v_k , \quad (5.43)$$

$$\approx \left[-b \frac{d}{d\tau} \delta(\tau - \tau_0) + \frac{\Delta z'}{z_0} \delta(\tau - \tau_0) + \dots \right] v_k , \quad (5.44)$$

where the dots denotes terms that do not contribute upon integration over the infinitely small region around τ_0 , and $\Delta z' \equiv z'|_{\tau_0^+}^{\tau_0^-}$. Because $z' = aHz(1 + \eta/2 - s)$, we have $z'|_{\tau_0^+}^{\tau_0^-} = aHz|_{\tau_0^+}^{\tau_0^-}$. Integrating (5.44) once and twice, we get the two boundary conditions for v_k ,

$$v_k|_{\tau_0^+} - v_k|_{\tau_0^-} = -bv_k|_{\tau_0^-} , \quad (5.45)$$

and

$$v_k'|_{\tau_0^+} - v_k'|_{\tau_0^-} = -baHv_k|_{\tau_0^-} . \quad (5.46)$$

Matching (5.37) and (5.38) we get

$$C_1 = \left[1 - \left(\frac{1}{2} + \frac{i}{2x_0} \right) b - \left(\frac{1}{8} - \frac{5i}{4x_0} \right) b^2 \right] e^{ibx_0} \quad (5.47)$$

$$C_2 = \left[\frac{ib}{2x_0} + \left(\frac{1}{2} - \frac{5i}{4x_0} \right) b^2 \right] e^{-i(2+b)x_0} \quad (5.48)$$

where we denote $x_0 = \tau_0 kc_s|_{\tau_0^-}$. The power spectrum is

$$P_{\mathcal{R}} = \frac{k^3}{2\pi^2} \frac{|v_k|^2}{z^2} \Big|_{\tau \rightarrow 0} = P_{\mathcal{R}0} \frac{|C_1 + C_2|^2}{1 + b} \quad (5.49)$$

where $P_{\mathcal{R}0} = H^2/(8\pi^2 \epsilon c_s|_{\tau_0^-})$. For small k , $x_0 \rightarrow 0$, so $P_{\mathcal{R}} \rightarrow P_{\mathcal{R}0}$ as expected. For large k , $P_{\mathcal{R}}$ is oscillating. The fact that such oscillation extends to infinitely large k is the artifact of approximating the change in c_s to be infinitely sharp. Such an approximation makes the potential barrier z''/z infinitely high, and introduces the v_2 component to all k modes. Realistically, the relaxation takes finite time ΔN_e , and the potential barrier in z''/z is finite. For modes with high frequency $kc_s \gg \sqrt{z''/z}$, it will not see the barrier in z''/z and the v_2 component is absent. Therefore, for the mode

$$k \gg \sqrt{\frac{z''}{z}} \sim k_0 \frac{\sqrt{b}}{\Delta N_e} \quad (5.50)$$

the oscillation is damped away. Here $k_0 \equiv aH/c_s$ is the mode number crossing the horizon at τ_0 .

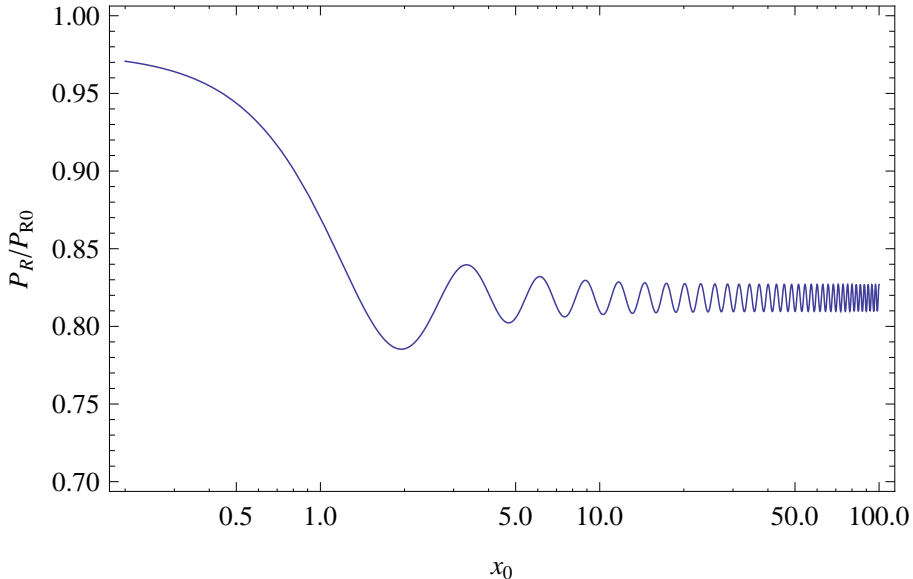


Figure 4: The approximate power spectrum, $P_{\mathcal{R}}$, as a function of $x_0 = kc_s\tau_0$, where τ_0 is the time of the feature, due to a θ function step with $b = 0.1$.

This power spectrum is illustrated in Fig. 4. The fact that the dip appears first for positive b can be seen analytically by taking the $bx_0 \ll 1$ limit,

$$P_{\mathcal{R}} \rightarrow P_{\mathcal{R}0} \left(1 - 2b + \frac{b}{x_0} \sin 2x_0 \right) . \quad (5.51)$$

Here we summarize several general properties from this analytical approximation. Firstly, the oscillation behavior in power spectrum can be understood as being due to the change of vacuum caused by the sharp feature. Such a change introduces a second (negative energy) component of v_k in addition to the original Bunch-Davis (positive energy) component. The superposition results in a oscillation in k -space. Secondly, the matching of the two set of solutions are done at the location of the sharp feature $x_0 = kc_s\tau_0 = k/k_0$, where $k_0 \equiv (-\tau_0 c_s)^{-1}$ is the wave number crossing the horizon at the moment of the feature τ_0 . The phase $2x_0$ gives the oscillation wavelength $\sim k_0/2$ in power spectrum model-independently. This implies that, in $\log k$ coordinate, the oscillation behavior looks similar for sharp features at different k_0 . Lastly, for a feature with finite width, the high frequency modes in the vacuum change adiabatically and remain in the Bunch-Davis vacuum. So the effect of the feature decay away for those modes. These conclusions apply for both the DBI and slow-roll case.

5.4 Numerical Analyses and Data Fitting

We have analyzed qualitatively the behavior of the power spectrum around the step. However, due to the non-trivial behavior of z''/z , the mode equation is hard to solve analytically in general. To better understand the effect of the sharp feature, we numerically

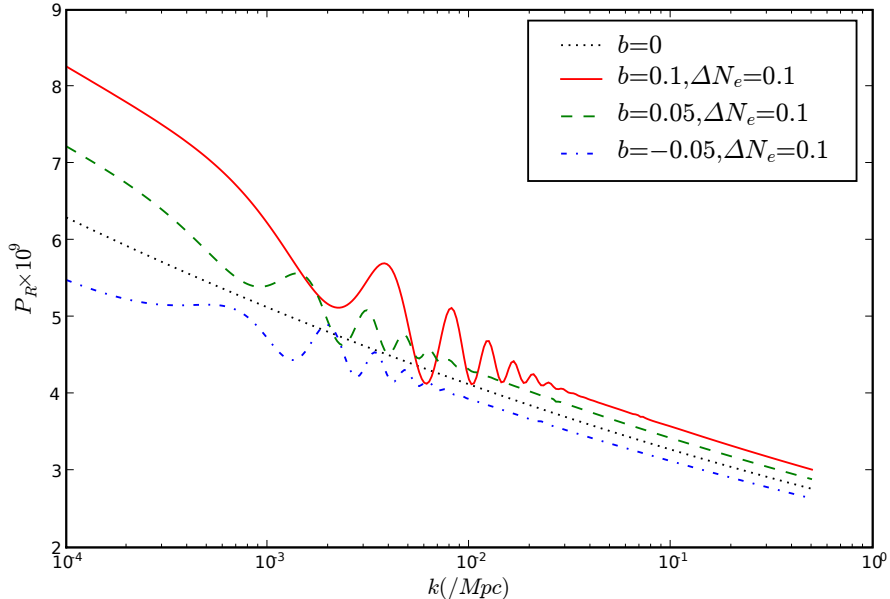


Figure 5: In the IR DBI scenario, we show the power spectrum, $P_{\mathcal{R}}$, when there is a sharp step in the warp factor. For the same step width ΔN_e , we show three cases with different step size b . The amplitude of the first dip and bump increases as we increase the step height b . A bump appears first for $b < 0$ while a dip appears first for $b > 0$.

solve the equation of motion Eq.(2.13), evolve the mode equation Eq.(3.2) starting from when the mode is deep inside the sound horizon ($c_s^2 k^2 \gg z''/z$) until the mode is frozen when stretched out of the sound horizon ($c_s^2 k^2 \ll z''/z$), and evaluate the power spectrum numerically using Eq.(3.4). The numerical calculation also has the advantage that it is not necessary to assume certain simplification conditions in Sec. 5.2, such as $b/\Delta N_e \gg 1$. Our major results are shown in Fig. 5 and Fig. 6.

Fig. 5 shows the step feature in the power spectrum $P_{\mathcal{R}}$ for steps with different height b , but same width ΔN_e . We see clearly that in the power spectrum, a dip appears first with positive b and a bump appears first with negative b , which agrees with our analytic result Eq.(5.49). However such a sequence gets less clear after projecting from k -space to l -space.

In Fig. 6 we explore the step feature with different step width ΔN_e . We see that the oscillation amplitude in $P_{\mathcal{R}}$ is quite insensitive to the step width d . By the same argument in our slow-roll analysis, the steps are sharp so that $\Delta N_e \ll 1$. The c_s and \dot{c}_s have reached their maximum values and so is the amplitude of the oscillation which is controlled by b as in (5.49).

In Fig. 7 we perform a χ^2 fit to the WMAP data. With one single step in the warp factor, we try to fit the $l \sim 20$ dip in WMAP temperature anisotropy. Here, instead of performing a full MCMC search for the best fit model, we only show an example to

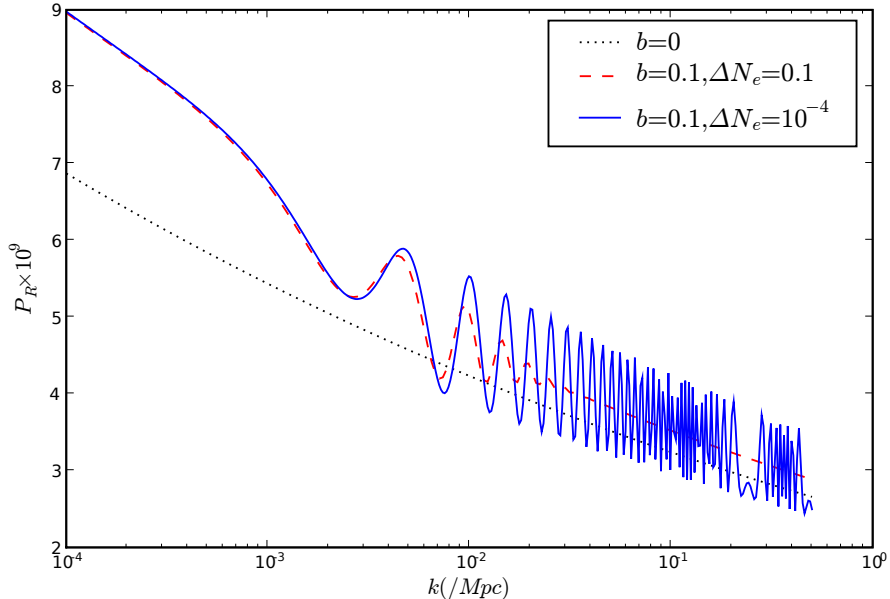


Figure 6: Same as Fig. 5, with the step size b fixed, we show two cases with different step width ΔN_e . Since in IR DBI model, the typical step width corresponds to $\Delta N_e \ll 1$, the dip and bump in the power spectrum is not sensitive to d . The width of the step affects only the range of oscillation in $P_{\mathcal{R}}$.

illustrate how the local step feature improves the quality of data fit. The example we show in Fig. 7 has the IR DBI model parameters $n_B = 6761$, $N_B = 4.315 \times 10^9$, $n_A h_A^4 = 0.01035$, $m_s/g_s^{1/4} = 2.567 \times 10^{-9} M_p$, $\beta = 4.021$, and the step parameters are $\Delta N_e = 0.105$ and $b = -0.35$. The step model, with likelihood \mathcal{L} , $-2 \ln \mathcal{L} = 5347.16$ when compared to WMAP 3-year temperature and polarization data [4, 5, 45, 46], has a better fit to the data, $\Delta \chi^2 = -2.76$, over the best-fit scenario with constant running of the spectral index, also shown. In light of the four extra degrees of freedom³ determining the cascade power spectrum in comparison to the fiducial running model, however, this improvement in χ^2 is not statistically significant.

We also find that a positive b is not favored by data, so the first dip in the k -space does not necessarily transform into a clear dip in the l -space. Numerically we find that to fit the $l \sim 20$ dip, we need $|b| \sim 0.3$. However, if we take $b = +0.3$, it gives too much power on large scale, more than that is allowed by data.

The reason that the glitch appears to be less sharper than that in slow-roll case is the following. In DBI inflation, a step in warp factor not only causes oscillation in power spectrum, but also changes the asymptotic speed-limit of the inflaton. So in addition to glitches, it also introduces a step in the power spectrum. Both amplitudes are controlled by

³Three of them specify the location, height and width of the step, another one is from IR DBI (versus LCDM).

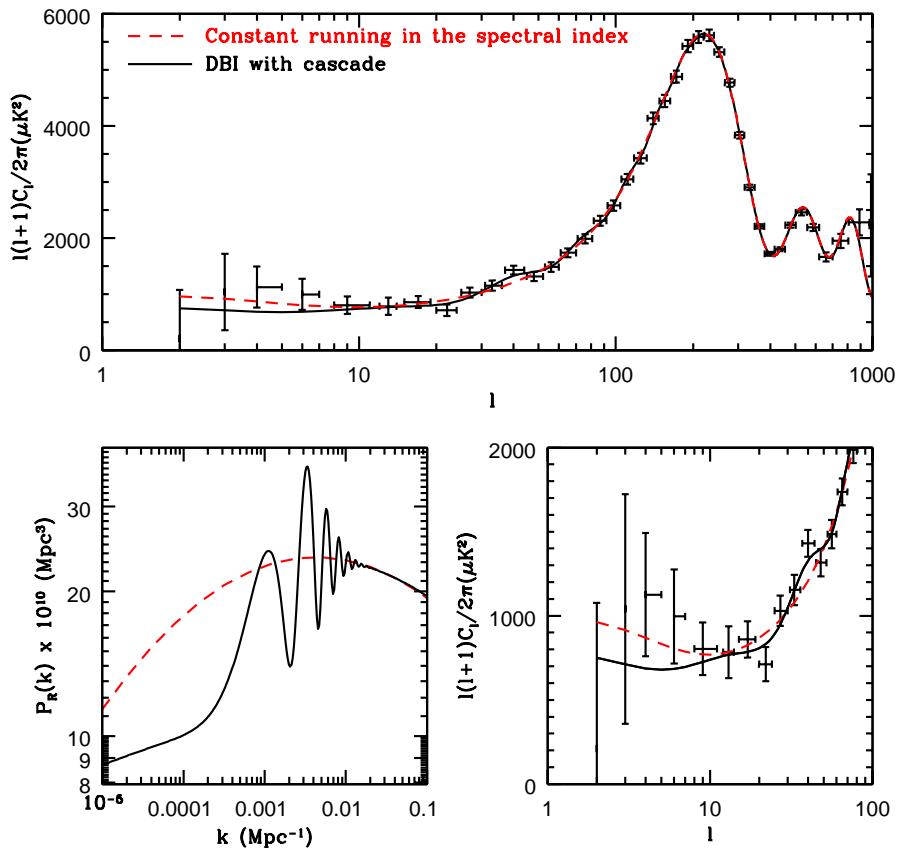


Figure 7: The CMB temperature power spectrum (top) and initial power spectrum (bottom left) in the presence of a step in the warp factor (full black line) and a best-fit scenario with constant running in the spectral index (red dashed line). The presence of large scale features in the cascade spectrum (bottom right) lead to an improved fit with the WMAP 3-year data of $\Delta\chi^2 = -2.76$ over the model with constant running in the spectral index.

the relative height of the step b . It is more difficult to generate a sharp glitch while keeping the latter effect compatible with data. While in slow-roll case, asymptotic velocities of the inflaton is not affected by a local step in potential. In this sense, for DBI inflation the glitches in power spectrum can be made sharper if one introduces a bump (or anything that does not change the asymptotic behaviors of the warp factor) instead of a step in the warping.

We should also point out that $|b| \sim 0.3$ gives a step much larger than that given by Eq.(2.9)⁴, which typically goes like $1/p^3$ with $p \gg 1$. This means that if we take the steps generated by the duality cascade, most probably we will not see any observable effects in the power spectrum. However, as we estimated in Eq. (5.34), the non-Gaussianities

⁴It is possible that duality cascade will generate large steps if we take $p \sim 1$. However, the perturbative analysis of the warp factor breaks down with $p \sim 1$, and we do not have any analytic control in that regime.

associated with the step can be very large depending on parameters in Eqs. (A.5) and (C.10). This can leave distinctive features detectable by experiments.

5.5 Closely Spaced Steps

We have been mainly concentrated on features that are sharp enough and well-separated (by at least one e-fold). We also see that there are parameter space where the feature is not sharp enough to show up in the CMB as observable signatures. In this case, the step is no longer important individually; but if there are parameter space such that, within one e-fold, the branes can go over many such small steps, a different kind of large non-Gaussianities can be generated through the “resonance mechanism” [47]. These closely spaced small steps induce small but high frequency oscillations of the background evolution in ϵ , $\tilde{\eta}$ and s . This oscillation can resonant with the mode functions u_k when the mode is still within the horizon. As a result of this resonance, the non-Gaussianity integration picks up a large contribution while the two-point function is only slightly affected. This non-Gaussianity has different signatures from the sharp feature case [47].

In slow-roll model, the condition to achieve this resonance mechanism relies on the shape of the potential. Naively, since we already have a series of steps, we can increase the tilt of the potential to make the branes roll faster so they come across many steps in one e-fold. Realistically, one needs to make sure that such a tilt will not significantly reduce the already-tuned total number of e-folds.

In IR DBI model, as we have discussed at the beginning of Sec. 5, there is actually a quite natural parameter space that such a condition can be satisfied, $1 > g_s > 10^{-3}$. We leave a more detailed study to a future publication.

6. Remarks

The analysis of the step feature in inflation in comparison with WMAP data has been carried out for large field models, specifically the quadratic chaotic inflationary model where the inflaton field starts at values much bigger than the Planck mass ($\phi > 15M_{\text{pl}}$) and then decreases to zero. In brane inflation, the inflaton being the position of the brane, is bounded by the size of the flux compactification volume, and so typically $\phi \ll M_{\text{pl}}$. This requires a generalized analysis, which is carried out here. In the IR DBI model, the behavior of the inflaton is further modified due to the DBI kinetic term. We have studied the properties and the signatures of the steps in warp factor and see that typically the effect on the power spectrum is much smaller, but non-Gaussianities can be much larger. So non-Gaussianities becomes a more important tool to probe the sharp features in DBI inflation. Another likely scenario is when the steps are too close to show up as sharp features in the power spectrum. Their presence is expected to show up in the bi- and tri-spectra. It is important to study this case further.

We end with some remarks on two broader aspects on brane inflation. In this paper we considered brane inflation as an effective one-field model driven by a potential in the radial direction. The location of the brane in each of the compact directions (one radial and five angular) is represented by a scalar field – brane inflation is therefore multi-field

in nature. Multi-field models can be decomposed into adiabatic and isocurvature fields, respectively describing motion along, and perpendicular to, an evolutionary trajectory in field space, where sharp features, such as sudden turns, in the trajectory can give rise to the interconversion of adiabatic and isocurvature modes [48, 49, 50]. The introduction of isocurvature perturbations can significantly modify the primordial power spectrum, and hence tight constraints on their contributions can be placed from observed CMB and large scale structure spectra [51, 52]. It will be interesting to see if these effects can be realized in brane inflation models.

In brane inflation, there are a number of possible sources of non-Gaussianities: (1) Even for a single $D3$ brane case, the inflaton is actually a six component field, namely, the radial mode plus the five angular modes. The angular modes are massless in the simplest scenario, though in general they are expected to pick up small masses. This is a multi-field inflation, where non-Gaussianity may arise; (2) the DBI action; (3) cosmic strings and their cosmic evolution, and (4) step-like behavior. In this paper, we focus on the step-like behavior due to the warp geometry, and its possible detection. If more than one source of non-Gaussianity are present, it will be important to disentangle them, for example via bi- and tri-spectra. In this sense, brane inflation can be very rich.

Acknowledgments

We thank Hiranya Peiris for providing the MCMC chain. We thank Richard Easter, Hassan Firouzjahi, Eiichiro Komatsu, Eugene Lim, Liam McAllister, Sarah Shandera, Gary Shiu and Eva Silverstein for valuable discussions. XC, HT and JX would like to thank the Kavli Institute for Theoretical Physics in China and the organizers of the ‘‘String Theory and Cosmology’’ program for warm hospitality. The work of RB is supported by the National Science Foundation under grants AST-0607018 and PHY-0555216. XC is supported by the US Department of Energy under cooperative research agreement DEFG02-05ER41360. The work of GH, SHT and JX is supported in part by the National Science Foundation under grant PHY-0355005.

A. The Warp factor

Let us consider the structure in the warp metric $h(r)$ that rescales masses, where

$$ds^2 = h^2(r)(-dt^2 + a(t)^2 d\mathbf{x}^2) + h^{-2}(r)(dr^2 + r^2 ds_5^2)$$

For the KS throat, we have the approximate Klebanov-Tseytlin solution [15]

$$h^{-4}(r) = \frac{27\pi\alpha'^2 g_s}{4r^4} \left(N + \frac{3g_s M^2}{2\pi} [\ln(r/R) + 1/4] \right), \quad (\text{A.1})$$

where, with the volume of $T^{1,1} \sim S^3 \times S^2$ given by $v\pi^3 = 16\pi^3/27$,

$$R^4 = 4\pi\alpha'^2 g_s N/v = \frac{27\pi\alpha'^2 g_s N}{4} \quad (\text{A.2})$$

and M is the RR-flux wrapping S^3 while $K = N/M$ is the orthogonal NS-NS-flux. The locations of duality transitions in the KS throat are given by

$$r_l = R \exp\left(-\frac{2l\pi}{3g_s M}\right). \quad (\text{A.3})$$

Note that the constant piece N in (A.1) is determined by the boundary condition. We see that the effective $D3$ -brane charge is given by

$$N_{\text{eff}} = N + \frac{3g_s M^2}{2\pi} \ln(r/R) \quad (\text{A.4})$$

so that at $r = r_l$, $N_{\text{eff}} = N - lM = K - l$. The term with $1/4$ factor is introduced to ensure that the warp factor $h^4(r)$ is monotonic for $R \geq r \geq r_K$.

The size of the step at $r = r_p$ in the warp factor $h(r)$ for large $p < K$ (where $r = r_{K+1}$ is at the edge of the throat) is estimated perturbatively to be (with string coupling g_s valued at the step),

$$\frac{\Delta h(r_p)}{h(r_p)} = \frac{h_>(r_p) - h_<(r_p)}{h(r_p)} \simeq \left(\frac{3g_s M}{2\pi}\right) \frac{1}{p^3}. \quad (\text{A.5})$$

where $h_>(r_p)$ is the warp factor at $r \geq r_p$ and $h_<(r_p)$ that at $r \leq r_p$. The widths of the steps are estimated in Appendix C. This series of steps leads to a cascading feature in the warp factor. So, in general, we expect this multi-step feature to be generic; as we approach the infrared (decreasing r), the step size grows (as p decreases). The spacings between steps are roughly equal as a function of $\ln r$ for large p .

In another throat, it is entirely possible that the leading $\Delta h(r_p)/h(r_p)$ appears at a different order, say p^{-2} instead of p^{-3} . It is also possible that $\Delta h(r_p)/h(r_p)$ can be negative, instead of positive, so $h(r)$ is ‘‘saw-like’’ instead of a cascade.

Here we write down the warp factor with steps given in [19] for a flow including only s number of steps starting from some location of duality transition at $r = r_{l_0}$; i.e, in the range $r_{l_0-1} < r < r_{l_0+s}$. The warp factor in this case can be written as

$$h^{-4}(r) \simeq h^{-4}(l_0, r) + \frac{27\pi\alpha'^2}{4r^4} \sum_{l=l_0}^{l_0+s-1} \left[g_s p_l M \left(\frac{3g_s M}{8\pi} \right) \times \frac{1}{2p_l^3} \left(1 + \tanh\left[\frac{r_l - r}{qr_l}\right] \right) \right], \quad (\text{A.6})$$

where $p_l \equiv K - (l - 1)$ and $h^{-4}(l_0, r)$ is given by

$$h^{-4}(l_0, r) \simeq \frac{27\pi\alpha'^2}{4r^4} \left[g_s N + \frac{3g_s^2 M^2}{2\pi} \left[\ln\left(\frac{r}{r_0}\right) + \frac{1}{4} \right] - \left(\frac{3g_s^2 M^2}{2\pi} \left[\ln\left(\frac{r}{r_{l_0}}\right) + \frac{1}{4} \right] \left[\frac{3g_s M}{\pi} \ln\left(\frac{r_{l_0-1}}{r_0}\right) + (2l_0 - 3) - \frac{3g_s M}{8\pi} \right] - \frac{9g_s^3 M^3}{4\pi^2} \left[\ln\left(\frac{r}{r_0}\right) + 2\left(\ln\left(\frac{r}{r_0}\right)\right)^2 + \frac{1}{4} \right] \right) \frac{1}{K - (l_0 - 1)} \right]. \quad (\text{A.7})$$

Note that the size of the step in $h^{-4}(r)$ at $r = r_l$ is

$$h^{-4}(l, r_l) - h^{-4}(l+1, r_l) \simeq -\frac{27\pi\alpha'^2 g_s N_{\text{eff}}}{4r_l^4} \left(\frac{3g_s M}{8\pi} \right) \frac{1}{p_l^3}, \quad (\text{A.8})$$

where $N_{\text{eff}} = N - (l-1)M = p_l M$ is the effective $D3$ -branes charge for the flow from the $(l-1)^{\text{th}}$ to the l^{th} duality transition point.

B. The z''/z in Slow Roll Case

In the presence of a feature like the step in the potential, the motion of the inflaton is divided into three phases: attractor before the step, acceleration within the step, and relaxation after the step. During the attractor phase, the inflaton moves along with the slow-roll attractor determined by the flat potential. In the acceleration phase, the inflaton gets accelerated by the local steep potential due to the step, and deviate away from the attractor solution. In the relaxation phase, the potential is flat again and the inflaton motion relaxes back to the slow-roll attractor due to Hubble friction.

Since Hubble friction is responsible for damping the deviation from slow-roll attractor, it is natural to expect that the relaxation time for $\dot{\phi}$ is of order H^{-1} or $\mathcal{O}(1)$ e-fold, and the same for $\epsilon, \tilde{\eta}$. However, the sharp change in z''/z takes place within a period much shorter than $\mathcal{O}(1)$ e-folds. To see this, we first express z''/z in terms of inflation parameters,

$$\begin{aligned} \frac{z''}{z} &= 2a^2 H^2 \left(1 - \frac{1}{2}\epsilon - \epsilon^2 + \frac{3}{4}\tilde{\eta} + \epsilon\tilde{\eta} + \xi^2 \right) \\ &\approx 2a^2 H^2 \left(1 + \frac{3}{4}\tilde{\eta} + \xi^2 \right), \end{aligned} \quad (\text{B.1})$$

where in the last line we have ignored the ϵ term since $\epsilon \ll 1$ in small field brane inflation models. The definitions of ϵ and $\tilde{\eta}$ follow the main text and ξ^2 is defined the following way

$$\xi^2 \equiv \frac{d^3\phi}{dt^3} \frac{1}{2H^2\dot{\phi}}. \quad (\text{B.2})$$

We can use the following equation of motion to eliminate the term $d^3\phi/dt^3$ in ξ^2 ,

$$\ddot{\phi} + 3H\dot{\phi} + \frac{dV}{d\phi} = 0. \quad (\text{B.3})$$

We then get

$$\xi^2 = -\frac{V''(\phi)}{2H^2} + 3\epsilon - \frac{3}{4}\tilde{\eta} \approx -\frac{V''(\phi)}{2H^2} - \frac{3}{4}\tilde{\eta}. \quad (\text{B.4})$$

Combining (B.1) and (B.4), we get

$$\frac{z''}{z} \approx 2a^2 H^2 \left(1 - \frac{V''(\phi)}{2H^2} \right). \quad (\text{B.5})$$

The result (B.5) is very useful in determining the relaxation time of z''/z . We see that the sharp feature in z''/z vanishes once $V''(\phi)$ goes back to normal, which only requires that

ϕ has moved across the step. Since the potential is very steep at the step, it only takes $\Delta N_e \ll 1$ e-folds for ϕ to move across. So z''/z relaxes much faster than ϵ , η and ξ^2 . When z''/z goes back to the attractor behavior, ϵ , η and ξ^2 still needs a few more e-folds to relax. Both are important to observational quantities.

C. Estimate the width of the steps

C.1 The width from Seiberg duality

The running of the two coupling constants g_1 and g_2 behave as

$$\frac{1}{g_{1,2}^2} = \pm \frac{3M}{8\pi^2} \ln \frac{\Lambda}{\mu} + \frac{1}{g_0^2} . \quad (\text{C.1})$$

The constant g_0 and the scale Λ are chosen such that at $\mu = \Lambda$, $g_1 = g_2 \equiv g_0$. In terms of the string coupling g_s , $g_0^2 = 8\pi g_s e^\Phi$, because

$$\frac{8\pi^2}{g_1^2} + \frac{8\pi^2}{g_2^2} = \frac{2\pi}{g_s e^\Phi} . \quad (\text{C.2})$$

The duality cascade happens when one of coupling, for example g_1 , becomes large. We denote such a coupling to be g_{SD} , which we expect to be of order one. The corresponding scale is

$$\mu_{SD} = \Lambda e^{\frac{8\pi^2}{3M}(\frac{1}{g_0^2} - \frac{1}{g_{SD}^2})} . \quad (\text{C.3})$$

The scale where one of the coupling hits infinity is

$$\mu_{1\infty} = \Lambda e^{\frac{8\pi^2}{3Mg_0^2}} , \quad (\text{C.4})$$

$$\mu_{2\infty} = \Lambda e^{-\frac{8\pi^2}{3Mg_0^2}} . \quad (\text{C.5})$$

So μ_∞ is the location of the transition wall, and μ_{SD} characterize its thickness. Therefore the width of the step is

$$\Delta\mu_{SD} = 2|\mu_{1\infty} - \mu_{SD}| , \quad (\text{C.6})$$

and the separation between the two steps is

$$|\mu_{1\infty} - \mu_{2\infty}| . \quad (\text{C.7})$$

Their ratio is

$$\frac{\Delta\mu_{SD}}{|\mu_{1\infty} - \mu_{2\infty}|} \approx \frac{8\pi^2}{g_{SD}^2} g_s e^\Phi . \quad (\text{C.8})$$

In terms of the distance r , the separation between the step l and $l+1$ is $2\pi r_l/3g_s M$. So the width of the step is

$$\Delta r_{SD} \approx \frac{16\pi^2}{3g_{SD}^2} \frac{r_l}{M} . \quad (\text{C.9})$$

In IR DBI inflation it is also convenient to write such a width in terms of the e-folds that brane spends crossing the width of the step. From the attractor solution $r \approx R^2/|t|$ and the fact that the speed-limit does not change much across the step, we get

$$\Delta N_e^{SD} \approx \frac{16\pi^2 N_e}{3g_{SD}^2 M}, \quad (\text{C.10})$$

where N_e is the e-fold to the end of DBI inflation at the location of the step.

C.2 The width from multiple brane spreading

In the multi-throat brane inflation scenario [13], inflaton branes are almost always generated in a large number. A typical generation mechanism can be the flux-antibrane annihilation. Once they are created at the end of the annihilation process, they can have different velocities. This introduces a spread in the mobile brane position. In this subsection, we estimate such a width. We express it in terms of e-folds $\Delta N_e^{\text{spread}}$.

The time-delay between the fastest brane and the static brane is the time period that the potential accelerates the brane from $\dot{\phi} = 0$ to the speed-limit ϕ^2/\sqrt{N} . Such an acceleration can be approximately described by

$$\ddot{\phi} = V'(\phi) = m^2 \phi. \quad (\text{C.11})$$

Consider initially, at $t = 0$, $\dot{\phi}_{min} = 0$ and $\phi_{min} = \sqrt{T_3} r_{min} = \sqrt{N} h_{min}/R$. At $t = \Delta t$, $\dot{\phi} = \phi^2/\sqrt{N}$. Here N and R are the charge and scale of the throat, respectively. We can therefore solve for Δt assuming $m\Delta t \ll 1$. Further, using $m \sim H$, we get

$$\Delta N_e^{\text{spread}} = H\Delta t \approx \frac{h_{min}}{HR}. \quad (\text{C.12})$$

For a long throat, the minimum warp factor is typically determined by the Hubble deformation as a result of the dS space back-reaction. In Ref. [36, 38], it is estimated to be $h_{min} \sim HR/\sqrt{N}$. So

$$\Delta N_e^{\text{spread}} \sim \frac{1}{\sqrt{N}}. \quad (\text{C.13})$$

Comparing (C.10) and (C.13), we see that generically $\Delta N_e^{SD} > \Delta N_e^{\text{spread}}$, although the relation can change for special parameters. The common feature is that both of them are almost invariant for different steps.

References

- [1] A. H. Guth, *The Inflationary Universe: A Possible Solution To The Horizon And Flatness Problems*, Phys. Rev. D **23**, 347 (1981).
- [2] A. D. Linde, *A New Inflationary Universe Scenario: A Possible Solution Of The Horizon, Flatness, Homogeneity, Isotropy And Primordial Monopole Problems*, Phys. Lett. B **108**, 389 (1982);
A. Albrecht and P. J. Steinhardt, *Cosmology For Grand Unified Theories With Radiatively Induced Symmetry Breaking*, Phys. Rev. Lett. **48**, 1220 (1982).
- [3] G. F. Smoot *et al.*, *Structure in the COBE DMR first year maps*, Astrophys. J. **396**, L1 (1992);
C. L. Bennett *et al.*, *4-Year COBE DMR Cosmic Microwave Background Observations: Maps and Basic Results*, Astrophys. J. **464**, L1 (1996), astro-ph/9601067.
- [4] G. Hinshaw *et al.* [WMAP Collaboration], *Three-year Wilkinson Microwave Anisotropy Probe (WMAP) observations: Temperature analysis*, Astrophys. J. Suppl. **170**, 288 (2007) [arXiv:astro-ph/0603451].
- [5] D. N. Spergel *et al.* [WMAP Collaboration], *Wilkinson Microwave Anisotropy Probe (WMAP) three year results: Implications for cosmology*, astro-ph/0603449.
- [6] R. Bean, D. J. H. Chung and G. Geshnizjani, *Reconstructing a general inflationary action*, arXiv:0801.0742 [astro-ph].
- [7] S.-H. H. Tye, *Brane inflation: String theory viewed from the cosmos*, hep-th/0610221.
- [8] G. R. Dvali and S.-H. H. Tye, *Brane inflation*, Phys. Lett. **B450** (1999) 72, hep-ph/9812483.
- [9] C. P. Burgess, M. Majumdar, D. Nolte, F. Quevedo, G. Rajesh and R. J. Zhang, *The inflationary brane-antibrane universe*, JHEP **0107**, 047 (2001) [arXiv:hep-th/0105204];
G. R. Dvali, Q. Shafi and S. Solganik, *D-brane inflation*, hep-th/0105203.
- [10] S. B. Giddings, S. Kachru, and J. Polchinski, *Hierarchies from fluxes in string compactifications*, Phys. Rev. **D66** (2002) 106006, hep-th/0105097 ;
S. Kachru, R. Kallosh, A. Linde, and S. P. Trivedi, *De sitter vacua in string theory*, Phys. Rev. **D68** (2003) 046005, hep-th/0301240.
- [11] S. Kachru, R. Kallosh, A. Linde, J. Maldacena, L. McAllister, and S. P. Trivedi, *Towards inflation in string theory*, JCAP **0310** (2003) 013, hep-th/0308055
- [12] E. Silverstein and D. Tong, *Scalar speed limits and cosmology: Acceleration from D-cceleration*, Phys. Rev. D **70**, 103505 (2004) [arXiv:hep-th/0310221].
- [13] X. Chen, *Multi-throat brane inflation*, Phys. Rev. D **71**, 063506 (2005) [arXiv:hep-th/0408084].
- [14] I. R. Klebanov and M. J. Strassler, *Supergravity and a confining gauge theory: Duality cascades and chib-resolution of naked singularities*, JHEP **08** (2000) 052, hep-th/0007191;
- [15] I. R. Klebanov and A. A. Tseytlin, *Gravity duals of supersymmetric $su(n) \times su(n+m)$ gauge theories*, Nucl. Phys. **B578** 123 (2000), hep-th/0002159;
- [16] A. Dymarsky, I. R. Klebanov, and N. Seiberg, *On the moduli space of the cascading $su(m+p) \times su(p)$ gauge theory*, JHEP **01** (2006) 155, hep-th/0511254.
- [17] N. Seiberg, *Electric-magnetic duality in supersymmetric nonabelian gauge theories*, Nucl. Phys. **B435** (1995) 129–146, hep-th/9411149.

- [18] M. J. Strassler, *The duality cascade*, [hep-th/0505153](#).
- [19] G. Hailu and S.-H. H. Tye, *Structures in the gauge/gravity duality cascade*, *JHEP* **08** (2007) 009, [[hep-th/0611353](#)].
- [20] S. Franco, A. Hanany and A. M. Uranga, *Multi-flux warped throats and cascading gauge theories*, *JHEP* **0509**, 028 (2005) [[arXiv:hep-th/0502113](#)].
- [21] J. A. Adams, G. G. Ross and S. Sarkar, *Multiple inflation*, *Nucl. Phys. B* **503**, 405 (1997) [[arXiv:hep-ph/9704286](#)].
- [22] S. M. Leach and A. R. Liddle, *Inflationary perturbations near horizon crossing*, *Phys. Rev. D* **63**, 043508 (2001) [[arXiv:astro-ph/0010082](#)].
- [23] S. M. Leach, M. Sasaki, D. Wands and A. R. Liddle, *Enhancement of superhorizon scale inflationary curvature perturbations*, *Phys. Rev. D* **64**, 023512 (2001) [[arXiv:astro-ph/0101406](#)].
- [24] P. Hunt and S. Sarkar, *Multiple inflation and the WMAP 'glitches'*, *Phys. Rev. D* **70**, 103518 (2004) [[arXiv:astro-ph/0408138](#)]; *Multiple inflation and the WMAP 'glitches' II. Data analysis and cosmological parameter extraction*, [arXiv:0706.2443](#) [[astro-ph](#)].
- [25] J. A. Adams, B. Cresswell and R. Easther, *Inflationary perturbations from a potential with a step*, *Phys. Rev. D* **64** (2001) 123514, [astro-ph/0102236](#).
- [26] H. V. Peiris *et al.* [WMAP Collaboration], *First year Wilkinson Microwave Anisotropy Probe (WMAP) observations: Implications for inflation*, *Astrophys. J. Suppl.* **148**, 213 (2003) [[arXiv:astro-ph/0302225](#)].
- [27] L. Covi, J. Hamann, A. Melchiorri, A. Slosar and I. Sorbera, *Inflation and WMAP three year data: Features have a future!*, *Phys. Rev. D* **74** (2006) 083509, [astro-ph/0606452](#); J. Hamann, L. Covi, A. Melchiorri and A. Slosar, *New constraints on oscillations in the primordial spectrum of inflationary perturbations*, [arXiv:astro-ph/0701380](#).
- [28] X. Chen, R. Easther and E. A. Lim, *Large non-Gaussianities in single field inflation*, *JCAP* **0706**, 023 (2007) [[arXiv:astro-ph/0611645](#)].
- [29] E. Komatsu *et al.* [WMAP Collaboration], *First Year Wilkinson Microwave Anisotropy Probe (WMAP) Observations: Tests of Gaussianity*, *Astrophys. J. Suppl.* **148**, 119 (2003) [[arXiv:astro-ph/0302223](#)].
- [30] M. Alishahiha, E. Silverstein and D. Tong, *DBI in the sky*, *Phys. Rev. D* **70**, 123505 (2004) [[arXiv:hep-th/0404084](#)].
- [31] X. Chen, *Running non-Gaussianities in DBI inflation*, *Phys. Rev. D* **72**, 123518 (2005) [[arXiv:astro-ph/0507053](#)].
- [32] D. Baumann and L. McAllister, *A microscopic limit on gravitational waves from D-brane inflation*, *Phys. Rev. D* **75**, 123508 (2007) [[arXiv:hep-th/0610285](#)].
- [33] R. Bean, S. E. Shandera, S.-H. H. Tye and J. Xu, *Comparing Brane Inflation to WMAP*, *JCAP* **0705**, 004 (2007) [[arXiv:hep-th/0702107](#)].
- [34] H. V. Peiris, D. Baumann, B. Friedman and A. Cooray, *Phenomenology of D-Brane Inflation with General Speed of Sound*, *Phys. Rev. D* **76**, 103517 (2007) [[arXiv:0706.1240](#)] [[astro-ph](#)].
- [35] R. Bean, X. Chen, H. V. Peiris and J. Xu, *Comparing Infrared Dirac-Born-Infeld Brane Inflation to Observations*, [arXiv:0710.1812](#) [[hep-th](#)].

- [36] X. Chen, *Inflation from warped space*, JHEP **0508**, 045 (2005) [arXiv:hep-th/0501184].
- [37] M. x. Huang and G. Shiu, *The inflationary trispectrum for models with large non-Gaussianities*, Phys. Rev. D **74**, 121301 (2006) [arXiv:hep-th/0610235].
- [38] X. Chen and S.-H. H. Tye, *Heating in brane inflation and hidden dark matter*, JCAP **0606**, 011 (2006) [arXiv:hep-th/0602136].
- [39] X. Chen, *Cosmological rescaling through warped space*, Phys. Rev. D **71**, 026008 (2005) [arXiv:hep-th/0406198].
- [40] X. Chen, S. Sarangi, S.-H. H. Tye and J. Xu, *Is brane inflation eternal?*, JCAP **0611**, 015 (2006) [arXiv:hep-th/0608082].
- [41] X. Chen, M. x. Huang, S. Kachru and G. Shiu, *Observational signatures and non-Gaussianities of general single field inflation*, JCAP **0701**, 002 (2007) [arXiv:hep-th/0605045].
- [42] A. R. Brown, S. Sarangi, B. Shlaer and A. Weltman, *A Wrinkle in Coleman-De Luccia*, arXiv:0706.0485 [hep-th].
- [43] J. M. Maldacena, *Non-Gaussian features of primordial fluctuations in single field*, JHEP **0305**, 013 (2003) [arXiv:astro-ph/0210603].
- [44] D. Seery and J. E. Lidsey, *Primordial non-gaussianities in single field inflation*, JCAP **0506**, 003 (2005) [arXiv:astro-ph/0503692].
- [45] L. Page *et al.* [WMAP Collaboration], *Three year Wilkinson Microwave Anisotropy Probe (WMAP) observations: Polarization analysis*, Astrophys. J. Suppl. **170**, 335 (2007) [arXiv:astro-ph/0603450].
- [46] N. Jarosik *et al.* [WMAP Collaboration], *Three-year Wilkinson Microwave Anisotropy Probe (WMAP) observations: Beam profiles, data processing, radiometer characterization and systematic error limits*, Astrophys. J. Suppl. **170**, 263 (2007) [arXiv:astro-ph/0603452].
- [47] X. Chen, R. Easther and E. A. Lim, *Generation and Characterization of Large Non-Gaussianities in Single Field Inflation*, arXiv:0801.3295 [astro-ph].
- [48] D. H. Lyth and A. Riotto, *Generating the curvature perturbation at the end of inflation in string theory*, Phys. Rev. Lett. **97**, 121301 (2006) [arXiv:astro-ph/0607326].
- [49] F. Vernizzi and D. Wands, *Non-Gaussianities in two-field inflation*, JCAP **0605**, 019 (2006) [arXiv:astro-ph/0603799].
- [50] D. A. Easson, R. Gregory, D. F. Mota, G. Tasinato and I. Zavala, *Spinflation*, arXiv:0709.2666 [hep-th];
M. x. Huang, G. Shiu and B. Underwood, *Multifield DBI Inflation and Non-Gaussianities*, arXiv:0709.3299 [hep-th].
- [51] R. Bean, J. Dunkley and E. Pierpaoli, *Constraining Isocurvature Initial Conditions with WMAP 3-year data*, Phys. Rev. D **74**, 063503 (2006) [arXiv:astro-ph/0606685].
- [52] R. Keskitalo, H. Kurki-Suonio, V. Muhonen and J. Valiviita, *Hints of Isocurvature Perturbations in the Cosmic Microwave Background?*, JCAP **0709**, 008 (2007) [arXiv:astro-ph/0611917].